ANNALS OF PHYSICS 233, 214–247 (1994)

Effects of the Electron–Phonon Interaction on the Cyclotron Resonance of Parabolic Quantum Wells in a Tilted Magnetic Field

R. HAUPT

Institut für Festkörpertheorie und Theoretische Optik, Friedrich-Schiller-Universität Jena, Max-Wien-Platz 1, D-07743 Jena, Germany

AND

L. WENDLER

Fachbereich Physik, Martin-Luther-Universität Halle, Friedemann-Bach-Platz 6, D-06108 Halle, Germany

Received August 4, 1993

We study in detail the interaction of electrons confined in one spatial direction in a parabolic quantum well with longitudinal-optical (LO) phonons, in a tilted magnetic field. The polaron correction to the electron levels and the polaron cyclotron mass are calculated using second-order perturbation theory. We present analytic and numerical results for the energy levels and the polaron cyclotron mass in dependence on the strength and the tilt angle of the applied magnetic field. It is shown that the electron–phonon induced corrections of the electron levels and, especially, the polaron cyclotron mass are very sensitive according to the tilt angle. For the case of an in-plane magnetic field it depends on the ratio of the confinement energy and the LO phonon energy whether cyclotron resonance results in a resonant magnetopolaron or not. © 1994 Academic Press, Inc.

I. INTRODUCTION

The development of epitaxial layer growth techniques and the advances in high-resolution submicrometer lithography have initiated a broad range of fundamental research activities in many fields of semiconductor physics. This progress makes it possible to fabricate semiconductor nanostructures which are precise in atomic scale and in which the carrier motion is quantum-confined in one, two, or three spatial directions.

In quasi-two-dimensional (Q2D) systems, i.e., heterojunctions and quantum wells (QW), the carrier motion is quasi-free parallel to the heterointerfaces but, according to the size-quantization, quantum-confined within a narrow channel perpendicular to the heterointerfaces (growth-direction). Therefore, Q2D systems are typified by an energy spectrum consisting of discrete levels in growth direction,

0003-4916/94 $9.00

the electric subbands, with typical energy separations of $\Delta\mathscr{E} \approx 20 \cdots 200$ meV for electrons and a free motion dispersion within the perpendicular plane.

One of the challenging topics of current interest involves systems of further reduced dimensionality: Q1D quantum-well wires (QWW) and Q0D quantum dots (QD). QWW's and QD's have been prepared by starting from Q2D systems employing nanometer techniques or directly by molecular-beam epitaxy, using macrosteps on semiconductor surfaces.

In the past few years, attention has been focused not only to the Q1D and Q0D systems but also on remotely doped parabolic quantum wells (PQW). PQW's are very interesting physical systems. In remotely doped wide PQW's it is possible to synthezise an almost three-dimensional electron gas with much weaker electron-impurity interactions than in conventional doped bulk semiconductors [1–9]. Further, in wide PQW's, it might be possible to observe broken-symmetry ground-states that have been predicted [10–12] for the three-dimensional electron gas at low densities in an external magnetic field. Experimental work on PQW's has been done on magnetotransport [2–4], on far-infrared (FIR) optical spectroscopy [5–7], and on photoluminescence excitation spectroscopy. It has been shown theoretically [13, 14] that in an initial bare ideal PQW the FIR absorption spectrum is independent of the number of electrons in the well, and it is also independent of the electron–electron interaction. Generalizing this result to the case of an applied magnetic field in a general direction, long-wavelength FIR optical perturbation can cause transitions only at the two frequencies that correspond to exact excitations in the center-of-mass motion of the electron gas [14]. This is called the generalized Kohn's theorem. Experiments [5, 7] show the possibility of growing PQW's that have optical spectra with two strong peaks. Extra peaks arise if departures from the ideal parabolicity of the initial bare potential are present. For the case of zero magnetic field [15, 16] and for nonvanishing magnetic field [17] the optical spectra have been calculated for wells that deviate from perfect parabolicity.

Usually, PQW's are fabricated from polar semiconductors. In polar semiconductors optical phonons are present which interact with the electrons, quantum-confined in the PQW's. Hence, the energy levels of an electron are modified by electron–phonon interaction (EPI). In a strong quantizing magnetic field the energy levels are modified by polaronic effects in the following manner: (i) they are shifted to lower energy; (ii) the slopes of the energy levels versus magnetic field are changed because of the mass renormalization of the electron; (iii) the energy levels do not cross the energy level formed by the lowest level plus one optical phonon and hence a splitting of these two levels occurs; and (iv) the levels are pinned to the energy of that virtual level (lowest level plus one optical phonon) in high magnetic fields. The EPI renormalizes the electron energy and mass, induces a non-parabolicity in the energy dispersion, and therefore forms a quasi-particle, the polaron. The polaron mass is usually experimentally determined by cyclotron resonance. In such an experiment the separation of adjacent energy levels is measured as a function of the magnetic field B. Therefore, in polar semiconductors the cyclotron resonance frequency $\omega_c^* = eB/m_c^*$, with m_c^* as the polaron cyclotron

mass, is renormalized by the interaction of the electrons with the optical phonons. Two different situations are commonly distinguished in 3D bulk and Q2D systems: the nonresonant magnetopolaron in low magnetic fields ($\omega_c \ll \omega_L$) and the resonant magnetopolaron in quantizing magnetic fields if the cyclotron frequency ω_c approximately equals the longitudinal optical phonon frequency ω_L. For the 3D bulk and the Q2D magnetopolaron considerable work has been done.

Polarons have been extensively studied both theoretically and experimentally in 3D systems [18, 19], including the magnetic field dependence of the electron–phonon correction to the energy of the Landau levels [20]. To study experimentally polaronic effects a very successful magneto-optical method is the cyclotron resonance [21, 22]. In general, polaronic effects in bulk semiconductor systems are well described by one-polaron theories [22]. This is valid because in undoped 3D semiconductors the electron density is usually relatively small ($\approx 10^{13}\,\mathrm{cm}^{-3}$ in GaAs) which leads to a Fermi energy $E_F \ll k_B T$ and, the electrons satisfy Boltzmann statistics. The mostly used way to calculate the polaron correction to the cyclotron resonance frequency or mass is to calculate the polaron correction to the energy levels of the electron where the EPI is usually treated within a perturbation schema. This is justified because the electron–phonon coupling strength is weak (for GaAs the coupling constant is $\alpha = 0.07$). Then the cyclotron resonance frequency can be obtained from the energy difference between two levels. There is still a different approach to calculate the polaron correction. This is the calculation of the magneto-optical absorption spectrum. To calculate the dynamical conductivity mostly the so-called memory function approach is used. Larsen calculated the electron–phonon corrections of the two lowest Landau levels in the weak-magnetic field limit and in the resonant case [23, 20]. Lindemann *et al.* [21] calculated the electron–phonon induced corrections of the lowest Landau levels using an improved Wigner–Brillouin perturbation theory which gives the correct pinning behaviour of the excited level. The influence of the intermediate and strong EPI on the first two Landau levels is discussed by Larsen [20], Peeters and Devreese [24]. Peeters and Devreese [25] calculated the Landau level corrections using second-order perturbation theory for all Landau levels and arbitrary magnetic field, but energies below the LO phonon continuum.

Theoretical model calculations [25–28] predict, that for an ideal 2D electron system, the one-polaron effects should be enhanced in comparison to 3D systems by factors 2–3. Das Sarma and Madhukar [26] calculated the polaronic Landau level corrections in the resonant region $\omega_c \simeq \omega_L$ using the so-called resonance approximation. Because of the complete quantized situation in Q2D systems there is no phonon continuum and hence, the splitting of the cyclotron-resonance line is observable. Further, Larsen [27] and Das Sarma [28] studied the 2D weak-coupling polaron in the presence of a small magnetic field. Peeters and Devreese [25] extended these studies to arbitrary magnetic fields and all Landau levels. Polaron effects in Q2D electron systems have been observed in many cyclotron resonance experiments on GaAs-$Ga_{1-x}Al_xAs$ heterostructures [29–32] and on InSb inversion layers [33, 34]. The available experimental data indicated Q2D polaron effects

which were both reduced [29–32, 35], comparable [36], and enhanced [33, 37] with respect to those in bulk systems. However, in most Q2D systems used in these experiments the 2D electron channel has a finite width and the electron density is typically $\sim 10^{11} \cdots 10^{12}\,\mathrm{cm}^{-2}$, corresponding to a 3D electron density of $\sim 10^{17} \cdots 10^{18}\,\mathrm{cm}^{-3}$. The resulting Fermi energy fulfils $E_F \gg k_B T$ and the electrons satisfy Fermi–Dirac statistics. Therefore, 2D one-polaron theories are not necessarily valid. It has been realized that in order to explain theoretical the experimental results it is necessary to take into account the non-zero width of the Q2D electron layer, i.e., to consider both the wave function and subband effect [27, 38–40]. Furthermore, it is shown to be necessary to take into account many-particle effects, like dynamical screening of the EPI and Landau-level occupation effects arising from Fermi–Dirac statistics. Both, the finite width of the electron channel [38–40] and the many-particle effects [41, 42] reduce the strength of the EPI. The up to now developed theory [42] has been successful in describing the energy dependence of the cyclotron effective mass in GaAs heterostructures at low temperatures and in magnetic fields up to 20T. Besides in cyclotron resonance experiments, Q2D polaron effects have been observed also in resonant tunneling [43]. Because semiconductor microstructures, such as heterostructures and quantum wells, are layered semiconductor systems, the spectrum of the optical phonons consists of confined LO phonons and interface phonons [44]. The effect of these Q2D phonons on the cyclotron resonance is calculated [45], but up to now not observed. Especially for InSb the conduction band nonparabolicity becomes important in the polaron physics [38, 34, 46].

It was shown very recently for Q1D systems [47] that it depends on the ratio of the confinement energy to the phonon energy, whether a resonant magnetopolaron case is possible or not. This is also true for Q0D magnetopolarons [48]. It is found [48] that the polaronic effects increase as the dimensionality is reduced.

In this paper we investigate the influence of the EPI on the electron energy levels of PQW's in a tilted magnetic field. Further, we calculate the polaron cyclotron mass. The electron–phonon correction is calculated within second-order perturbation theory for arbitrary magnetic fields. Numerical results are presented for $Ga_{1-x}Al_xAs$ PQW's with $Ga_{1-y}Al_yAs$ barriers ($x < y$).

II. Energy Levels in a Tilted Magnetic Field

The unperturbed system, a single electron confined in an ideal parabolic quantum well in the z-direction in the presence of a quantizing magnetic field $\mathbf{B} = (0, B\sin\Theta, B\cos\Theta)$, tilted at an angle Θ with respect to the z-direction in the y–z plane, is described by the Hamiltonian

$$H_e = \frac{1}{2m_e}(\mathbf{p} + e\mathbf{A})^2 + V(\mathbf{x}), \tag{1}$$

where we ignore the Zeeman spin-splitting. In this equation m_e is the effective conduction band-edge mass, $\mathbf{A}$ is the vector potential with $\mathbf{B}=\nabla\times\mathbf{A}$, $V(\mathbf{x})=V(z)=m_e\Omega^2 z^2/2$ is the parabolic confinement potential and the electron charge is $-e$. For the vector potential we use the gauge $\mathbf{A}=(z\sin\Theta-y\cos\Theta,0,0)B$. The single-particle wave function is

$$\langle \mathbf{x} \mid \Psi \rangle = \Psi(\mathbf{x}) = \frac{1}{\sqrt{L_x}} e^{ik_x x}\Phi(y,z), \tag{2}$$

where we have applied Born–von Kármán periodic boundary conditions in the x-direction and k_x is the electron wave vector component in this direction. We suppose spin degeneracy, but omit the spin eigenvalue and coordinate. Using this wave function in the Schrödinger equation of the Hamiltonian, given in Eq. (1), it reads

$$\left\{\frac{\hbar^2}{2m_e}\left[k_x^2-\frac{\partial^2}{\partial y^2}-\frac{\partial^2}{\partial z^2}\right]+\frac{m_e}{2}\left[\omega_c^2 y^2\cos^2\Theta+(\Omega^2+\omega_c^2\sin^2\Theta)z^2\right]\right.$$
$$\left.-\hbar k_x\omega_c[y\cos\Theta-z\sin\Theta]-m_e\omega_c^2 yz\sin\Theta\cos\Theta\right\}\Phi(y,z)=\mathscr{E}\Phi(y,z), \tag{3}$$

where $\omega_c=eB/m_e$ is the cyclotron frequency.

To solve this partial differential equation it is necessary to remove the term $\propto yz$ by a linear transformation. This simplification of the Hamiltonian is possible through a change of the coordinates $y\to y'$ and $z\to z'$ corresponding to a rotation of the coordinate system y–z of an angle α_r with respect to the y-axis [49, 50]:

$$y=y'\cos\alpha_r-z'\sin\alpha_r, \qquad z=y'\sin\alpha_r+z'\cos\alpha_r.$$

The rotation angle α_r is obtained from the condition that the term $\propto yz$ must vanish. Under this condition we obtain

$$\alpha_r=\frac{1}{2}\arctan\left[\frac{\omega_c^2\sin 2\Theta}{\Omega^2-\omega_c^2\cos 2\Theta}\right]. \tag{4}$$

After this transformation the Schrödinger equation reads

$$\left\{\frac{\hbar^2}{2m_e}\left[k_x^2-\frac{\partial^2}{\partial y'^2}-\frac{\partial^2}{\partial z'^2}\right]+\frac{m_e}{2}\left[\omega_y^2 y'^2+\omega_z^2 z'^2\right]\right.$$
$$\left.-\hbar k_x\omega_c[v_y y'+v_z z']\right\}\Phi(y',z')=\mathscr{E}\Phi(y',z'), \tag{5}$$

with

$$v_y^2=\frac{1}{2}\left[1-\frac{\omega_c^2-\Omega^2\cos 2\Theta}{\sqrt{\omega_c^4+\Omega^4-2\omega_c^2\Omega^2\cos 2\Theta}}\right]$$

and

$$v_z^2 = \frac{1}{2}\left[1 + \frac{\omega_c^2 - \Omega^2 \cos 2\Theta}{\sqrt{\omega_c^4 + \Omega^4 - 2\omega_c^2\Omega^2 \cos 2\Theta}}\right]. \tag{6}$$

The frequencies ω_y and ω_z are given by

$$\begin{aligned} \omega_y &= \{\tfrac{1}{2}[\omega_c^2 + \Omega^2 - (\omega_c^4 + \Omega^4 - 2\omega_c^2\Omega^2 \cos 2\Theta)^{1/2}]\}^{1/2}, \\ \omega_z &= \{\tfrac{1}{2}[\omega_c^2 + \Omega^2 + (\omega_c^4 + \Omega^4 - 2\omega_c^2\Omega^2 \cos 2\Theta)^{1/2}]\}^{1/2}. \end{aligned} \tag{7}$$

Introducing the quantities $l_y^2 = \gamma_y l_0^2$ and $l_z^2 = \gamma_z l_0^2$ with $\gamma_y = \omega_c/\omega_y$ and $\gamma_z = \omega_c/\omega_z$, where $l_0^2 = \hbar/(m_e\omega_c)$ is the magnetic length, Eq. (5) has the form

$$\begin{aligned} \Big\{\frac{\hbar^2 k_x^2}{2m_e}[1 - \mu_y^2 - \mu_z^2] - \frac{\hbar^2}{2m_e}\frac{\partial^2}{\partial y'^2} + \frac{m_e}{2}\omega_y^2(y' - Y_{k_x})^2 \\ - \frac{\hbar^2}{2m_e}\frac{\partial^2}{\partial z'^2} + \frac{m_e}{2}\omega_z^2(z' - Z_{k_x})^2\Big\}\Phi(y', z') = \mathscr{E}\Phi(y', z'), \end{aligned} \tag{8}$$

where $Y_{k_x} = \mu_y l_y^2 k_x$ and $Z_{k_x} = \mu_z l_z^2 k_x$ are the center coordinates of a shifted two-dimensional harmonic oscillator with the displaced centre at Y_{k_x} and Z_{k_x}. Here $\mu_y = \gamma_y v_y$ and $\mu_z = \gamma_z v_z$. Because $1 - \mu_y^2 - \mu_z^2 = 0$ is valid, we obtain the following eigenenergies of a single electron in a PQW in the presence of a tilted magnetic field:

$$\mathscr{E}_{N_y N_z} = \hbar\omega_y(N_y + \tfrac{1}{2}) + \hbar\omega_z(N_z + \tfrac{1}{2}), \qquad N_y, N_z = 0, 1, 2, \ldots. \tag{9}$$

The corresponding single-particle wave function is

$$\langle \mathbf{x} \mid N_y, N_z, k_x\rangle = \Psi_{N_y N_z k_x}(\mathbf{x}) = \frac{1}{\sqrt{L_x}} e^{ik_x x}\Phi_{N_y}(y' - Y_{k_x})\,\Phi_{N_z}(z' - Z_{k_x}), \tag{10}$$

with

$$y' = y\cos\alpha_r + z\sin\alpha_r, \qquad z' = -y\sin\alpha_r + z\cos\alpha_r$$

and

$$\begin{aligned} \Phi_{N_y}(y' - Y_{k_x}) = \frac{1}{\sqrt{2^{N_y} N_y!\,\pi^{1/2} l_y}} \\ \times \exp\left[-\frac{1}{2l_y^2}(y' - Y_{k_x})^2\right] H_{N_y}\left[\frac{1}{l_y}(y' - Y_{k_x})\right], \end{aligned} \tag{11a}$$

$$\begin{aligned} \Phi_{N_z}(z' - Z_{k_x}) = \frac{1}{\sqrt{2^{N_z} N_z!\,\pi^{1/2} l_z}} \\ \times \exp\left[-\frac{1}{2l_z^2}(z' - Z_{k_x})^2\right] H_{N_z}\left[\frac{1}{l_z}(z' - Z_{k_x})\right]. \end{aligned} \tag{11b}$$

$H_N(\xi)$ is the Hermite polynomial. Let us consider explicitly the two special cases of a perpendicular quantizing magnetic field ($\Theta = 0°$) and of an in-plane quantizing magnetic field ($\Theta = 90°$). For $\Theta = 0°$ the eigenvalues are

$$\mathscr{E}_{N_y N_z} = \hbar\omega_c(N_y + \tfrac{1}{2}) + \hbar\Omega(N_z + \tfrac{1}{2}) \tag{12}$$

and the corresponding single-particle wave function is given by

$$\Psi_{N_y N_z k_x}(\mathbf{x}) = \frac{1}{\sqrt{L_x}} e^{ik_x x} \Phi_{N_y}(y - Y_{k_x})\, \Phi_{N_z}(z), \tag{13}$$

where now $l_y = l_0$ and $l_z = l_\Omega$ and, therefore, $Y_{k_x} = l_0^2 k_x$ and $Z_{k_x} = 0$ with $l_\Omega^2 = \hbar/(m_e\Omega)$.

Since the energy eigenvalues $\mathscr{E}_{N_y N_z}$ are independent of the quantum number k_x for all angles $\Theta \neq 90°$, each energy level is degenerated. For a finite system the allowed values of the quantum number k_x are separated by $2\pi/L_x$ so that the total number N_L of k_x values which belongs to the same energy $\mathscr{E}_{N_y N_z}$ is

$$N_L = \frac{eB}{h} A; \qquad A = L_x L_y. \tag{14}$$

The degeneracy factor is identical to the number of flux quanta ($\Phi_0 = h/e$) within the area A.

This degeneracy is lifted for the special case of an in-plane quantizing magnetic field ($\Theta = 90°$). For this case we obtain

$$\mathscr{E}_{N_z}(k_x, k_y) = \frac{\hbar^2 k_x^2}{2\tilde{m}} + \frac{\hbar^2 k_y^2}{2m_e} + \hbar\tilde{\omega}_c\left(N_z + \frac{1}{2}\right) \tag{15}$$

and

$$\Psi_{N_z k_x k_y}(\mathbf{x}) = \frac{1}{\sqrt{A}} e^{i(k_x x + k_y y)} \Phi_{N_z}(z - Z_{k_x}), \tag{16}$$

where $\tilde{\omega}_c = (\omega_c^2 + \Omega^2)^{1/2}$ is the hybrid frequency, $\tilde{m} = m_e(\tilde{\omega}_c/\Omega)^2$ is the magnetic-field dependent kinetic mass, and now $l_z^2 = \hbar/(m_e\tilde{\omega}_c)$ which results in the centre coordinate $Z_{k_x} = \gamma_z l_z^2 k_x$ with $\gamma_z = \omega_c/\tilde{\omega}_c$. Therefore, for $\Theta = 90°$ the discrete quantum number N_y changes to the quasi-continuous wave vector component k_y and the degeneracy according k_x is lifted. Note, that the quasi-classical electron motion in the x–y plane now becomes anisotropic.

In Figs. 1a–g the unperturbed energy levels denoted by (N_y, N_z) of the states $|N_y, N_z, k_x\rangle$ for one electron in a perfect PQW are plotted as a function of the magnetic field for different angles Θ of the tilted magnetic field using the material parameters for GaAs. For the confinement frequency $\Omega/\omega_L = 0.5$ is used, where ω_L is the frequency of the longitudinal-optical (LO) phonon.

The special case of $\Theta = 0°$ is plotted in Fig. 1a. It is seen that for $B = 0$ the discrete subband structure $\mathscr{E}_{N_z}$ arises according to the size quantization in z-direction. For $B \neq 0$ the electron motion in the x–y plane also is quantized. As the result of this magnetic quantization the discrete Landau levels $\mathscr{E}_{N_y}$ of each size-quantized level $\mathscr{E}_{N_z}$ arise. For the perpendicular case ($\Theta = 0°$) the magnetic and size quantization are independent. Following, the Landau levels $\mathscr{E}_{N_y}$ are independent from the size-quantized levels $\mathscr{E}_{N_z}$ resulting in a possible level crossing for certain magnetic fields.

If one tilts the magnetic field with respect to the z-axis (see Fig. 1b) then the magnetic quantization in the plane perpendicular to the magnetic field direction and the size quantization couple with the result that the level crossing now is lifted [4, 5, 51]. This is called resonant subband-Landau level coupling (RSLC). For the special case of a perfect parabolic confinement in the z-direction most of the level crossing points are retained. Only for such magnetic fields where the cyclotron frequency ω_c is equal to the confinement frequency Ω is the level crossing lifted and anticrossing occurs. From Figs. 1b to 1f it is seen that with increasing angle Θ the resonance split gaps increase. Further, it is seen from Figs. 1a to 1g that for $\Theta = 0°$ each size-quantized level has its own ladder of Landau levels independent from the others. Tilting the magnetic field with respect to the z-axis each size-quantized level has a ladder of hybrid levels. For instance, the energy level (1, 0) hybridizes with (0, 1). With increasing angle the splitting of the hybrid levels increases and the width of the ladder is lowered. That means, the energy difference between the hybrid levels of each size-quantized level $\mathscr{E}_{N_z}$ is narrowed (see Fig. 1f for $\Theta = 85°$). For the in-plane case (Fig. 1g) the energy levels represent mixed subband-Landau levels (see Eq. (15)) with a magnetic field-dependent energy separation $\Delta\mathscr{E} = \hbar\tilde{\omega}_c$ similar to the energy levels of a parabolic QWW (see, for instance, Ref. [47]).

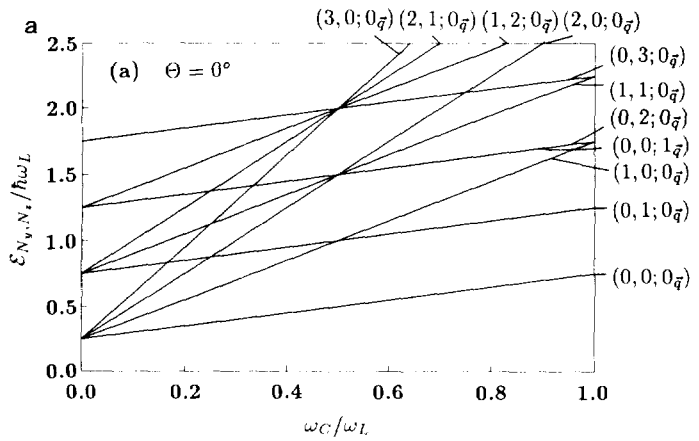

FIG. 1. The unperturbed energy levels $(N_y, N_z; n_{\mathbf{q}})$, composed of an electron in the energy level (N_y, N_z) and n LO phonons with the momentum $\hbar\mathbf{q}$ and the energy $\hbar\omega_L$, as a function of the magnetic field in a PQW with a confinement frequency of $\Omega/\omega_L = 0.5$ for different angles Θ. The thin line corresponds to the unperturbed level $(0, 0; 1_{\mathbf{q}})$.

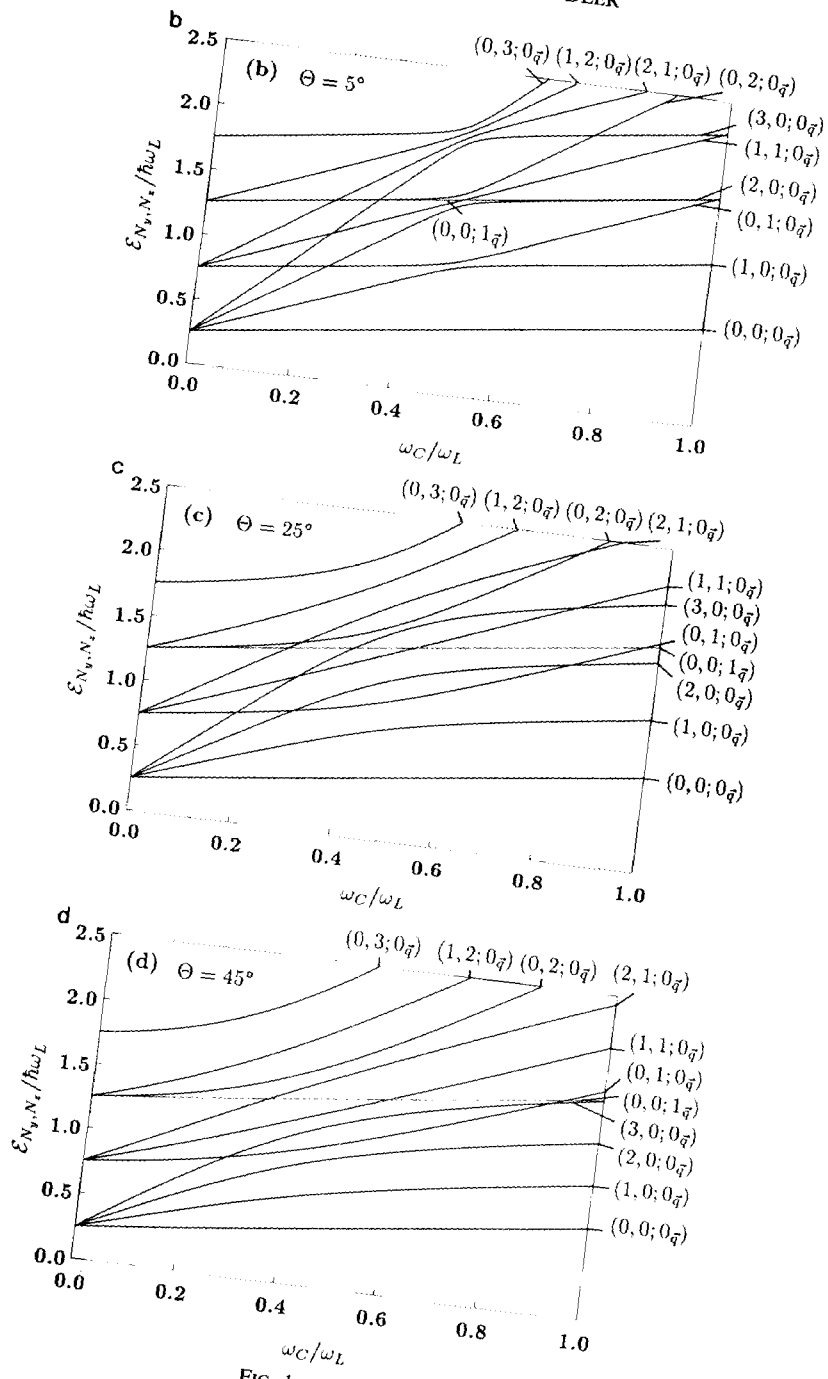

FIG. 1—*Continued.*

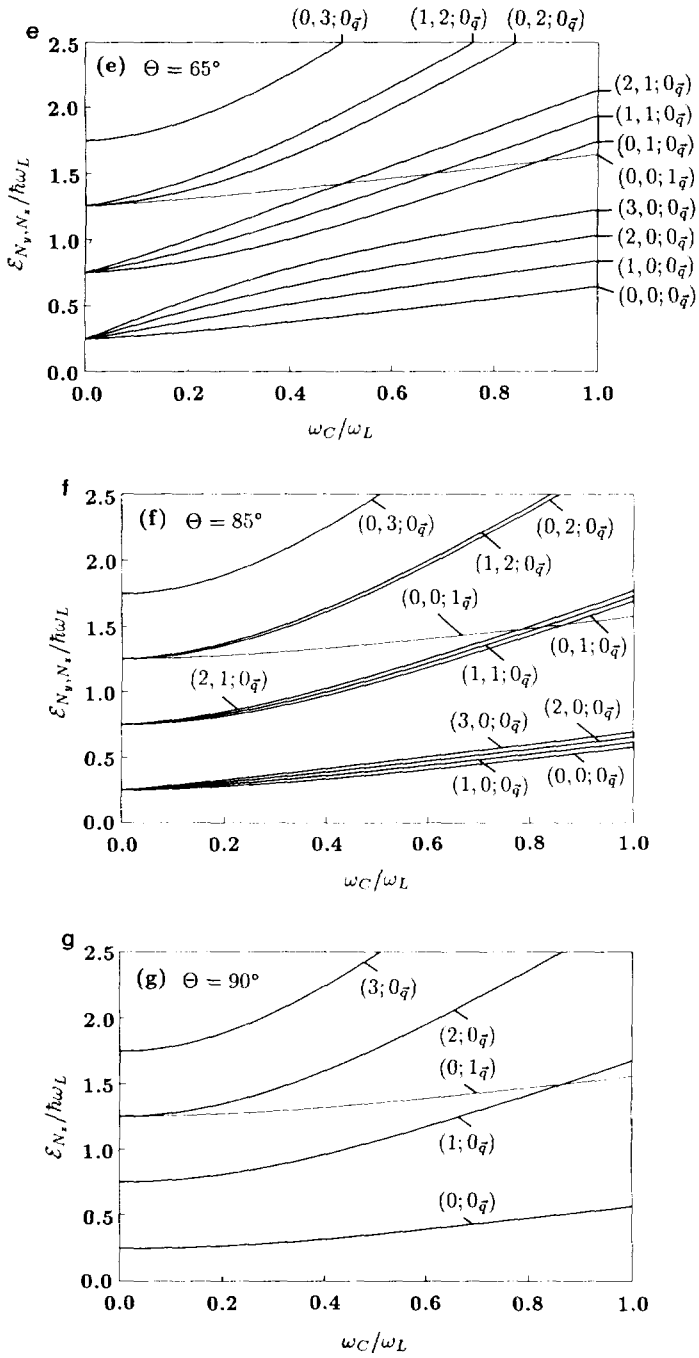

FIG. 1—*Continued.*

The character of these hybrid levels changes with the increasing magnetic field from subband-like to Landau-like levels. For the in-plane case the magnetic field is in the y-direction and quantizes the electron motion in the z-direction. In the y-direction the electron motion becomes quasi-free with typical quadratic dispersion. Without the parabolic potential in the z-direction the quantized motion in the x–z plane would result in the Landau levels $\mathscr{E}_N = \hbar\omega_c(N+\frac{1}{2})$. These levels are changed due to the presence of $V(z) = m_e\Omega^2 z^2/2$ to the mixed subband-Landau levels $\mathscr{E}_{N_z}(k_x) = \hbar^2 k_x^2/(2\tilde{m}) + \hbar\tilde{\omega}_c(N_z+\frac{1}{2})$ accompanied by a lifting of the degeneracy according to the wave vector component k_x. In a classical picture, the term $\hbar^2 k_x^2/(2\tilde{m})$ arises from the electrons which skip along the two edges of the potential due to the confinement potential and the Lorentz force.

If one includes the EPI in the consideration then the question arises, what is the effect of the EPI on these levels, especially on the resonance gaps. Furthermore, it is important to know how the cyclotron polaron mass changes in dependence on the strength of the magnetic field and in dependence on the tilt angle of the magnetic field with respect to the z-axis. In the next section we give an answer to these important questions.

III. Electron–Phonon Interaction

If an electron is placed in a polar semiconductor then it polarizes its surroundings. This dielectric polarization is connected with the vibration of the solid in an optical mode. Because only long-wavelength optical phonons are accompanied by large electric dipole moments and, hence, by large polarization fields, only these phonons interact with the electrons. Therefore, to describe the dielectric polarization, the crystal lattice is treated as a continuum. The dielectric continuum model is the basis of the polar or Fröhlich type of EPI [52]. This type of EPI describes the coupling of the macroscopic electric field with the charge of the electron. In a 3D bulk polar semiconductor the electrons only interact with the LO phonons [52], but in layered systems of polar semiconductors the electrons interact with modified LO and interface phonons [44, 53, 54]. For simplicity we will assume that the electrons inside of the PQW only interact with 3D bulk LO phonons. Neglecting the effects arising from the z-dependent varying Al content of the host material $Ga_{1-x}Al_xAs$, which produces the parabolic shape of the conduction band-edge of the PQW, the Hamiltonian of the EPI is the standard Fröhlich Hamiltonian [52]:

$$H_{ep} = \left(\frac{4\pi\alpha r_p(\hbar\omega_L)^2}{V_G}\right)^{1/2} \sum_{\mathbf{q}} e^{i\mathbf{q}\mathbf{x}} \frac{1}{|\mathbf{q}|} (a_L(\mathbf{q}) + a_L^+(-\mathbf{q})) \tag{17}$$

with

$$\alpha = \frac{1}{2}\frac{e^2}{4\pi\varepsilon_0 r_p}\left(\frac{1}{\varepsilon_\infty} - \frac{1}{\varepsilon_s}\right)\frac{1}{\hbar\omega_L}$$

the dimensionless 3D polaron coupling constant, $r_p = (\hbar/2m_e\omega_L)^{1/2}$ as the corresponding 3D polaron radius, ε_∞ and ε_s are the high frequency (optical) and the

static dielectric constant of the semiconductor containing the electrons, respectively; ε_0 is the permittivity of vacuum; $a_L(\mathbf{q})$ and $a_L^+(\mathbf{q})$ are the phonon destruction and creation operators, respectively; $\mathbf{q}=(q_x, q_y, q_z)$ is the 3D wave vector of the 3D bulk LO phonon; and V_G is the volume of the sample. The Hamiltonian of the magnetopolaron is given by

$$H_p = H_e + \sum_{\mathbf{q}} \hbar\omega_L (a_L^+(\mathbf{q})\, a_L(q) + \tfrac{1}{2}) + H_{\text{ep}}. \tag{18}$$

The first two terms represent the unperturbed electron and the LO phonon system, H_0, and $H_1 = H_{\text{ep}}$ is the electron–phonon interaction Hamiltonian.

The EPI forms from the electron in the presence of the LO phonons a new quasiparticle, the polaron, composed of an electron and the surrounding phonon cloud.

The energy levels of an electron are shifted over $\Delta E_{N_y, N_z}$ in the case $\Theta < 90°$ and $\Delta E_{N_z}(k_x, k_y)$ for $\Theta = 90°$ by the interaction with the LO phonons:

$$E_{N_y N_z} = \hbar\omega_y (N_y + \tfrac{1}{2}) + \hbar\omega_z (N_z + \tfrac{1}{2}) + \Delta E_{N_y N_z}, \tag{19a}$$

$$E_{N_z}(k_x, k_y) = \frac{\hbar^2 k_x^2}{2\tilde{m}} + \frac{\hbar^2 k_y^2}{2m_e} + \hbar\tilde{\omega}_c \left(N_z + \frac{1}{2}\right) + \Delta E_{N_z}(k_x, k_y). \tag{19b}$$

In this paper we only consider weakly polar semiconductors with $\alpha \ll 1$. This is the weak-coupling limit and so it is sufficient to consider perturbed states that contain no more than one LO phonon. Therefore, the energy shift is calculated using second-order perturbation theory. The energy shift of the level (N_y, N_z) in the case $\Theta < 90°$ and of the level (N_z, k_x, k_y) for $\Theta = 90°$ is given by

$$\Delta E_{N_y, N_z} = -\sum_{N_y', N_z' = 0}^{\infty} \sum_{\mathbf{q}} \frac{|M_{N_z' N_z}^{N_y' N_y}(\mathbf{q})|^2}{D_{N_z' N_z}^{N_y' N_y}}, \tag{20a}$$

$$\Delta E_{N_z}(k_x, k_y) = -\sum_{N_z' = 0}^{\infty} \sum_{\mathbf{q}} \frac{|M_{N_z' N_z}(\mathbf{q})|^2}{D_{N_z' N_z}^{k_x k_y}(q_x, q_y)}, \tag{20b}$$

where the matrix elements are $M_{N_z' N_z}^{N_y' N_y}(\mathbf{q}) = \langle N_y', N_z', k_x - q_x; 1_{\mathbf{q}} | H_{\text{ep}} | N_y, N_z, k_x; 0_{\mathbf{q}} \rangle$ and $M_{N_z' N_z}(\mathbf{q}) = \langle N_z', k_x - q_x, k_y - q_y; 1_{\mathbf{q}} | H_{\text{ep}} | N_z, k_x, k_y; 0_{\mathbf{q}} \rangle$. The ket $|N_y, N_z, k_x; n_{\mathbf{q}}\rangle = |N_y, N_z, k_x\rangle \otimes |n_{\mathbf{q}}\rangle$ describes an eigenstate of H_0 composed of an electron in the energy level (N_y, N_z) with a momentum $\hbar k_x$ and n LO phonons with the momentum $\hbar\mathbf{q}$ and the energy $\hbar\omega_L$ in the case $\Theta < 90°$, whereas the ket $|N_z, k_x, k_y; n_{\mathbf{q}}\rangle$ is an eigenstate of H_0 for $\Theta = 90°$ composed of an electron in the energy level (N_z) with the momentum $(\hbar k_x, \hbar k_y)$ and n LO phonons with the momentum $\hbar\mathbf{q}$ and the energy $\hbar\omega_L$. The corresponding level we call the n-phonon unperturbed level or the unrenormalized n-phonon magnetopolaron level as opposed to the renormalized level, the n-phonon magnetopolaron level, containing n LO phonons. Using the state vectors given above and the Hamiltonian, Eq. (17), the matrix elements are given explicitly by

$$|M_{N_z' N_z}^{N_y' N_y}(\mathbf{q})|^2 = \frac{4\pi\alpha r_p (\hbar\omega_L)^2}{V_G} \frac{1}{q^2} \frac{N_{y2}!}{N_{y1}!} a_y^{N_{y1} - N_{y2}} e^{-a_y}$$
$$\times |L_{N_{y2}}^{N_{y1} - N_{y2}}(a_y)|^2 \frac{N_{z2}!}{N_{z1}!} a_z^{N_{z1} - N_{z2}} e^{-a_z} |L_{N_{z2}}^{N_{z1} - N_{z2}}(a_z)|^2 \tag{21a}$$

with

$$a_y = \frac{l_y^2}{2}\mu_y^2\left(q_x^2 + \frac{1}{\mu_y^2}q_y^2\right), \qquad a_z = \frac{l_z^2}{2}\mu_z^2\left(q_x^2 + \frac{1}{\mu_z^2}q_z^2\right)$$

for the case $\Theta < 90°$ and

$$|M_{N_z'N_z}(\mathbf{q})|^2 = \frac{4\pi\alpha r_p(\hbar\omega_L)^2}{V_G}\frac{1}{q^2}\frac{N_{z2}!}{N_{z1}!}a_z^{N_{z1}-N_{z2}}e^{-a_z}|L_{N_{z2}}^{N_{z1}-N_{z2}}(a_z)|^2 \tag{21b}$$

with

$$a_z = \frac{l_z^2}{2}\gamma_z^2\left(q_x^2 + \frac{1}{\gamma_z^2}q_z^2\right)$$

for $\Theta = 90°$. Here $N_{y(z)1} = \max(N_{y(z)}, N'_{y(z)})$, $N_{y(z)2} = \min(N_{y(z)}, N'_{y(z)})$, and $q^2 = q_x^2 + q_y^2 + q_z^2$. $L_N^{N'}(\xi)$ is the associated Laguerre polynomial.

The energy dominator in Eq. (20a) for $\Theta < 90°$ is given by

$$D_{N_z'N_z}^{N_y'N_y} = \hbar\omega_L + \hbar\omega_y(N_y' - N_y) + \hbar\omega_z(N_z' - N_z) - \Delta_{N_yN_z}, \tag{22a}$$

and in Eq. (20b) for the case $\Theta = 90°$ by

$$D_{N_z'N_z}^{k_xk_y}(q_x, q_y) = \hbar\omega_L + \frac{\hbar^2}{2\tilde{m}}(q_x^2 - 2k_xq_x) + \frac{\hbar^2}{2m_e}(q_y^2 - 2k_yq_y) + \hbar\tilde{\omega}_c(N_z' - N_z) - \Delta_{N_z}(k_x, k_y), \tag{22b}$$

where the values $\Delta_{N_yN_z}$ and $\Delta_{N_z}(k_x, k_y)$ depend on the type of the perturbation theory which is used [21]: (i) $\Delta_{N_yN_z} = 0$ ($\Delta_{N_z}(k_x, k_y) = 0$) leads to the Rayleigh–Schrödinger perturbation theory (RSPT); (ii) $\Delta_{N_yN_z} = \Delta E_{N_yN_z}$ ($\Delta_{N_z}(k_x, k_y) = \Delta E_{N_z}(k_x, k_y)$) results in the Wigner–Brillouin perturbation theory (WBPT); and (iii) $\Delta_{N_yN_z} = \Delta E_{N_yN_z} - \Delta E_{00}^{\mathrm{RSPT}}$ ($\Delta_{N_z}(k_x, k_y) = \Delta E_{N_z}(k_x, k_y) - \Delta E_0^{\mathrm{RSPT}}(0, 0)$) gives the improved Wigner–Brillouin perturbation theory (IWBPT), with $\Delta E_{00}^{\mathrm{RSPT}}$ ($\Delta E_0^{\mathrm{RSPT}}(0, 0)$) is the weak-coupling electron–phonon correction to the electron ground-state energy, calculated within RSPT. For the ground state $\Delta E_{00}^{\mathrm{IWBPT}} = \Delta E_{00}^{\mathrm{RSPT}}$ ($\Delta E_0^{\mathrm{IWBPT}}(0, 0) = \Delta E_0^{\mathrm{RSPT}}(0, 0)$) is valid.

Introducing polaron units in Eq. (20) (energies are measured in units of $\hbar\omega_L$ and lengths are measured in units of the 3D polaron radius r_p), one obtains for the case $\Theta < 90°$,

$$\Delta E_{N_yN_z} = -\frac{4\pi\alpha}{V_G}\sum_{N_y', N_z' = 0}^{\infty}\sum_{\mathbf{q}}\frac{1}{q^2}\frac{1}{1 + \lambda_y^2(N_y' - N_y) + \lambda_z^2(N_z' - N_z) - \Delta_{N_yN_z}} * \frac{N_{y2}!}{N_{y1}!}a_y^{N_{y1}-N_{y2}}e^{-a_y}|L_{N_{y2}}^{N_{y1}-N_{y2}}(a_y)|^2\frac{N_{z2}!}{N_{z1}!} \times a_z^{N_{z1}-N_{z2}}e^{-a_z}|L_{N_{z2}}^{N_{z1}-N_{z2}}(a_z)|^2 \tag{23}$$

with

$$a_y = \left(\frac{\mu_y}{\lambda_y}\right)^2 \left(q_x^2 + \frac{1}{\mu_y^2} q_y^2\right), \qquad a_z = \left(\frac{\mu_z}{\lambda_z}\right)^2 \left(q_x^2 + \frac{1}{\mu_z^2} q_z^2\right),$$

and $\lambda_y^2 = \omega_y/\omega_L$, $\lambda_z^2 = \omega_z/\omega_L$.

For the two special cases of a perpendicular magnetic field ($\Theta = 0°$) and an in-plane magnetic field ($\Theta = 90°$) we obtain

(i) for $\Theta = 0°$, $\Delta E_{N_y N_z}$ is given by Eq. (23) with $a_y = (1/\lambda_y^2)(q_x^2 + q_y^2)$ and $a_z = (1/\lambda_z^2)\, q_z^2$, where $\lambda_y^2 = \xi = \omega_c/\omega_L$ and $\lambda_z^2 = \eta = \Omega/\omega_L$ ($\mu_y = 1$, $\mu_z = 0$).

(ii) For $\Theta = 90°$ it is valid that

$$\Delta E_{N_z}(k_x, k_y) = -\frac{4\pi\alpha}{V_G} \sum_{N_z'=0}^{\infty} \sum_{\mathbf{q}} \frac{1}{q^2} * \frac{1}{1 + (1-\gamma_z^2)(q_x^2 - 2k_x q_x) + (q_y^2 - 2k_y q_y) + \lambda_z^2 (N_z' - N_z) - \Delta_{N_z}(k_x, k_y)} * \frac{N_{z2}!}{N_{z1}!} a_z^{N_{z1} - N_{z2}} e^{-a_z} |L_{N_{z2}}^{N_{z1} - N_{z2}}(a_z)|^2 \tag{24}$$

with

$$a_z = \left(\frac{\gamma_z}{\lambda_z}\right)^2 \left(q_x^2 + \frac{1}{\gamma_z^2} q_z^2\right)$$

and $\lambda_z^2 = \tilde{\omega}_c/\omega_L$.

It is well known that the RSPT describes the ground-state correction for $\omega_c \to 0$ quite well, but it fails for the excited states, since it is possible that the denominator of Eq. (23) vanishes for certain ω_c. This is true because there exist always energy levels $(N_y, N_z; 0_{\mathbf{q}})$ crossing the energy level $(0, 0; 1_{\mathbf{q}})$ at that value ω_c^R, where the condition $\omega_L = N_y \omega_y + N_z \omega_z$ is fulfilled. For $\Theta \neq 90°$ such a level crossing takes place independent of the ratio between ω_L and Ω. But for $\Theta = 90°$ the energy level $(N_z, k_x = 0, k_y = 0; 0_{\mathbf{q}})$, only under the condition that $\omega_L > N_z \Omega$, crosses the energy level $(0, 0, 0; 1_{\mathbf{q}})$ at $\omega_c^R = [(\omega_L/N_z)^2 - \Omega^2]^{1/2}$. Under the condition $\omega_L \leqslant N_z \Omega$ no level crossing occurs. Hence, the in-plane case of $\Theta = 90°$ is very similar to the case of a parabolic QWW in a perpendicular magnetic field [47]. The only difference is the additional free dispersion in the y-direction for the electron in a PQW.

If resonance occurs, the EPI leads to a splitting of the degenerated levels. The levels are repelled from the level $(0, 0; 1_{\mathbf{q}})$ and pinned to the energy $\hbar\omega_L + \hbar\omega_y/2 + \hbar\omega_z/2 + \Delta E_{00}^{\mathrm{RSPT}}$. Only the IWBPT gives the correct pinning behaviour.

In Figs. 1a to 1g, in addition to the unperturbed electron levels $(N_y, N_z; 0_{\mathbf{q}})$, also the unrenormalized magnetopolaron level $(0, 0; 1_{\mathbf{q}})$ is plotted for $\eta = \Omega/\omega_L = 0.5$. From Figs. 1a to 1g it is seen that for $\Theta = 0°$ the resonance of the level $(1, 0; 0_{\mathbf{q}})$ with the level $(0, 0; 1_{\mathbf{q}})$ is at $\omega_c^R = \omega_L$ which defines the magnetic field $B_L = m_e \omega_L/e$. For this special case the subbands arising from the geometrical confinement in the z-direction and the Landau levels arising from the magnetic confinement in the x–y

plane are completely decoupled. For nonvanishing angle $\Theta \neq 0°$ RSLC occurs. This leads to the fact that now the resonance between the level $(0, 1; 0_q)$ and $(0, 0; 1_q)$ at $\omega_c^R = \omega_L \sqrt{\omega_L^2 - \Omega^2}/\sqrt{\omega_L^2 - \Omega^2 \cos^2 \Theta} < \omega_L$ occurs if $\Omega < \omega_L$ is valid.

Experimentally one obtains information about the levels by cyclotron resonance. In such an experiment one measures the energetic difference between the ground-state and an excited state of the electron if the transition is dipole-allowed and derives the corresponding polaron cyclotron mass in dependence on the strength of the magnetic field and the angle Θ. The dipole-allowed single-electron transitions are determined by the matrix elements of the dipole operator $\mathbf{p} = -e\mathbf{x}$ of a single electron. If one chooses the direction of the incident radiation and the direction of the magnetic field to be equal for any angle with $0° < \Theta < 90°$, both transitions $(0, 0; 0_q) \to (1, 0; 0_q)$ and $(0, 0; 0_q) \to (0, 1; 0_q)$ can be excited. This is true due to the RSLC arising from the coupled electron motion perpendicular and parallel to the PQW. Hence, both harmonic oscillators are excitable by an incident FIR radiation that is directed along the direction of the magnetic field with the result that this radiation is absorbed at ω_y and ω_z if one neglects the EPI. Contrary to the case $0° < \Theta < 90°$ discussed above, for a perpendicular magnetic field ($\Theta = 0°$) only the transition $(0, 0; 0_q) \to (1, 0; 0_q)$ can be measured and for an in-plane magnetic field ($\Theta = 90°$) only the transition $(0, 0, 0; 0_q) \to (1, 0, 0; 0_q)$ is measurable. The other transitions are not dipole-allowed.

Therefore, it is possible, using cyclotron resonance, to measure the transitions $(0, 0; 0_q) \to (1, 0; 0_q)$ and $(0, 0; 0_q) \to (0, 1; 0_q)$ and to determine the energy difference and the polaron cyclotron mass for these transitions.

Here, we will investigate the influence of the EPI in dependence on the magnetic field $\mathbf{B}$ for both dipole-allowed transitions $E_{00} \to E_{10}$ and $E_{00} \to E_{01}$. Hence, it is necessary to calculate the energy shifts ΔE_{00}, ΔE_{10}, and ΔE_{01}.

Transforming the sum over $\mathbf{q}$ into an integral and converting the denominator of Eq. (23) by the integral

$$\frac{1}{D^{N_y' N_y}_{N_z' N_z}} = \int_0^\infty dt \exp(-D^{N_y' N_y}_{N_z' N_z} t), \tag{25}$$

where $D^{N_y' N_y}_{N_z' N_z} > 0$ must be fulfilled, we obtain

$$\begin{aligned}
\Delta E_{00} = & -\frac{\alpha}{2\pi^2} \int_0^\infty dt\, e^{-(1-\Delta_{00})t} \\
& * \int_{-\infty}^{\infty} dq_y\, e^{-(1/\lambda_y^2)(1-\exp(-\lambda_y^2 t))\, q_y^2} \int_{-\infty}^{\infty} dq_z\, e^{-(1/\lambda_z^2)(1-\exp(-\lambda_z^2 t))\, q_z^2} \\
& * \int_{-\infty}^{\infty} dq_x \frac{1}{q_x^2 + q_y^2 + q_z^2} e^{-[(\mu_y^2/\lambda_y^2)(1-\exp(-\lambda_y^2 t)) + (\mu_z^2/\lambda_z^2)(1-\exp(-\lambda_z^2 t))]\, q_x^2}.
\end{aligned} \tag{26}$$

In Eq. (26) the sums over N_y' and N_z' are performed exactly. Now the integral over q_x can be calculated and polar coordinates are introduced in the $q_y - q_z$ plane, $q_y = q_\perp \cos\varphi$, $q_z = q_\perp \sin\varphi$, and $q_\perp = (q_y^2 + q_z^2)^{1/2}$, with the result that

$$\Delta E_{00} = -\frac{2\alpha}{\pi} \int_0^\infty dt\, e^{-(1-\Delta_{00})t} * \int_0^{\pi/2} d\varphi \int_0^\infty dq_\perp\, e^{b_0 q_\perp^2} \operatorname{erfc}[\sqrt{c}\, q_\perp] \tag{27}$$

with

$$b_0 = \left[\frac{\mu_y^2 - \cos^2\varphi}{\lambda_y^2} (1 - \exp(-\lambda_y^2 t)) + \frac{\mu_z^2 - \sin^2\varphi}{\lambda_z^2} (1 - \exp(-\lambda_z^2 t)) \right]$$

and

$$c = \frac{\mu_y^2}{\lambda_y^2} (1 - \exp(-\lambda_y^2 t)) + \frac{\mu_z^2}{\lambda_z^2} (1 - \exp(-\lambda_z^2 t)),$$

where $\operatorname{erfc}(x)$ is the complementary error function. According to the three possible different cases for b_0 we finally obtain

$$\Delta E_{00} = -\frac{\alpha}{\pi^{3/2}} \int_0^\infty dt\, e^{-(1-\Delta_{00})t} \int_0^{\pi/2} d\varphi \begin{cases} \dfrac{1}{\sqrt{b_0}} \ln \dfrac{\sqrt{c} + \sqrt{b_0}}{\sqrt{c} - \sqrt{b_0}}, & b_0 > 0, \\ \dfrac{2}{\sqrt{c}}, & b_0 = 0, \\ \dfrac{2}{\sqrt{-b_0}} \arctan \sqrt{-b_0/c}, & b_0 < 0. \end{cases} \tag{28}$$

Thus the ground-state energy correction is given by a two-dimensional integral.

It is interesting to consider the special cases of the perpendicular magnetic field ($\Theta = 0°$) and of the in-plane magnetic field ($\Theta = 90°$) explicitly. For $\Theta = 0°$ it is possible to perform the integral over φ analytically with the result that

$$\Delta E_{00} = -\frac{\alpha}{\pi^{1/2}} \int_0^\infty dt\, e^{-(1-\Delta_{00})t} \begin{cases} \dfrac{1}{\sqrt{f_\eta - f_\xi}} \ln \dfrac{\sqrt{f_\eta} + \sqrt{f_\eta - f_\xi}}{\sqrt{f_\xi}}, & \xi > \eta, \\ \dfrac{1}{\sqrt{f_\eta}}, & \xi = \eta, \\ \dfrac{1}{\sqrt{f_\xi - f_\eta}} \arcsin \sqrt{(f_\xi - f_\eta)/f_\xi}, & \xi < \eta, \end{cases} \tag{29}$$

where

$$f_\eta = \frac{1}{\eta}(1 - e^{-\eta t}), \qquad f_\xi = \frac{1}{\xi}(1 - e^{-\xi t}).$$

For the in-plane magnetic field ($\Theta = 90°$), we obtain the expression

$$\begin{aligned} \Delta E_0(k_x, k_y) = & -\frac{\alpha}{2\pi^2} \int_0^\infty dt\, e^{-(1 - \Delta_0(k_x, k_y))t} \\ & * \int_{-\infty}^{\infty} dq_y\, e^{-(\gamma_z^2/\lambda_z^2)(1 + \lambda_z^2 t(1/\gamma_z^2 - 1) - e^{-\lambda_z^2 t}) q_y^2 + 2(1 - \gamma_z^2) t k_y q_y} \\ & * \int_{-\infty}^{\infty} dq_z\, e^{-(1/\lambda_z^2)(1 - e^{-\lambda_z^2 t}) q_z^2} \int_{-\infty}^{\infty} dq_x \frac{e^{-t q_x^2 + 2t k_x q_x}}{q_x^2 + q_y^2 + q_z^2}. \end{aligned} \tag{30}$$

This expression can be expanded in a power series of k_x^2 and k_y^2: $\Delta E_0(k_x, k_y) = \Delta E_0(0, 0) + \partial \Delta E_0(k_x, 0)/\partial k_x^2|_{k_x = 0} * k_x^2 + \partial \Delta E_0(0, k_y)/\partial k_y^2|_{k_y = 0} * k_y^2 + \cdots$. The components of the magnetopolaron effective mass tensor $\tilde{m}^*$ and m_e^* for motion in the x–y plane are related to the second-order terms in the standard manner. The magnetopolaron ground-state correction is given by the term $\Delta E_0(0, 0)$:

$$\Delta E_0(0, 0) = -\frac{\alpha}{\pi^{1/2}} \int_0^\infty dt\, e^{-(1 - \Delta_0(0,0))t} \frac{1}{\sqrt{g_z}} \mathbf{F}(\arcsin \sqrt{g_z/t}, \gamma_z) \tag{31}$$

with

$$g_z = (1/\lambda_z^2)(e^{-\lambda_z^2 t} + \lambda_z^2 t - 1)$$

and $\mathbf{F}(a, b)$ is the elliptical integral of the first kind.

It gives a deeper insight into the effect of the EPI in a tilted magnetic field if one discusses the energy renormalization $\Delta E_{N_y N_z}$ in the limit of a weak magnetic field. If $\xi = \omega_c/\omega_L \ll 1$ is valid, nondegenerated perturbation theory, i.e., RSPT, is a good approximation and, therefore, one has $\Delta_{N_y N_z} = 0$.

If one expands the ground-state renormalization ΔE_{00} for the special case of a perpendicular magnetic field ($\Theta = 0°$) in a power series according to ξ, we obtain for the EPI correction from Eq. (29) for small magnetic fields:

$$\begin{aligned} \Delta E_{00} = & -\frac{\alpha}{\pi^{1/2}} \int_0^\infty dt\, e^{-t} \left\{ \frac{1}{\sqrt{g_\eta}} \arcsin \sqrt{g_\eta/t}\, \xi^0 \right. \\ & + \left[\frac{t^2}{4 g_\eta^{3/2}} \arcsin \sqrt{g_\eta/t} - \sqrt{f_\eta}\, t/4 g_\eta \right] \xi^1 \\ & \left. + \left[\frac{t^3(t + 8 f_\eta)}{96 g_\eta^{5/2}} \arcsin \sqrt{g_\eta/t} - \frac{\sqrt{f_\eta}\, t^2(7t + 2 f_\eta)}{96 g_\eta^2} \right] \xi^2 + \mathcal{O}(\xi^3) \right\} \end{aligned} \tag{32}$$

with $g_\eta = t - f_\eta$.

For the in-plane magnetic field ($\Theta = 90°$) we obtain for the EPI correction for small magnetic fields from Eq. (31):

$$\Delta E_0(0,0) = -\frac{\alpha}{\pi^{1/2}} \int_0^\infty dt\, e^{-t} \left\{ \frac{1}{\sqrt{g_\eta}} \arcsin \sqrt{g_\eta/t}\, \xi^0 \right.$$
$$+ \frac{1}{4\pi\eta^2\sqrt{t}} \int_0^{\pi/2} d\varphi \left[\frac{1}{1-\sin^2\varphi(g_\eta/t)} \left(\frac{\eta t f_\eta}{g_\eta} - 1 + 2\cot^2\varphi \right) \right.$$
$$\left. \left. - \frac{1}{\sin\varphi} \sqrt{t/g_\eta} \ln \frac{1+\sin\varphi\sqrt{g_\eta/t}}{1-\sin\varphi\sqrt{g_\eta/t}} \left(\frac{\eta t f_\eta}{g_\eta} - 1 + 2\cot^2\varphi \right) \right] \xi^2 + \mathcal{O}(\xi^4) \right\}. \tag{33}$$

The zero magnetic field limit of $\Delta E_{00}|_{\xi\to 0}$ for $\Theta = 0°$, given in Eq. (32), and of $\Delta E_0(0,0)|_{\xi\to 0}$ for $\Theta = 90°$, given in Eq. (33), yield the same result, which desribes the ground-state renormalization of a Q2D polaron in a PQW.

Now, we consider the energy shifts ΔE_{10} and ΔE_{01}. Transforming again in Eq. (23) the sum over $\mathbf{q}$ into an integral, converting the denominator by the integral, Eq. (25), and performing the sums over N_y' and N_z', it follows that

$$\Delta E_{10} = -\frac{\alpha}{2\pi^2} \int_0^\infty dt\, e^{-(1-\Delta_{10})t}$$
$$* \int_{-\infty}^\infty dq_y\, e^{-(1/\lambda_y^2)(1-\exp(-\lambda_y^2 t))q_y^2} \int_{-\infty}^\infty dq_z\, e^{-(1/\lambda_z^2)(1-\exp(-\lambda_z^2 t))q_z^2}$$
$$* \int_{-\infty}^\infty dq_x \frac{1}{q_x^2+q_y^2+q_z^2} e^{-[(\mu_y^2/\lambda_y^2)(1-\exp(-\lambda_y^2 t))+(\mu_z^2/\lambda_z^2)(1-\exp(-\lambda_z^2 t))]q_x^2}$$
$$* \left[1 + 4\frac{1}{\lambda_y^2} \sinh^2\left(\frac{\lambda_y^2 t}{2}\right) q_y^2 + 4\frac{\mu_y^2}{\lambda_y^2} \sinh^2\left(\frac{\lambda_y^2 t}{2}\right) q_x^2 \right]. \tag{34}$$

Now we can perform the integral over q_x and introduce polar coordinates again in the $q_y - q_z$ plane. Then Eq. (34) reads

$$\Delta E_{10} = -\frac{2\alpha}{\pi} \int_0^\infty dt\, e^{-(1-\Delta_{10})t} * \int_0^{\pi/2} d\varphi \int_0^\infty dq_\perp$$
$$\times \left[e^{b_0 q_\perp^2} * \operatorname{erfc}[\sqrt{c}\, q_\perp](1 - a_0 q_\perp^2) + \frac{a_1}{\sqrt{c}} e^{-b_1 q_\perp^2} q_\perp \right], \tag{35}$$

with

$$b_1 = c - b_0,$$
$$a_0 = \frac{4}{\lambda_y^2} \sinh^2\left(\frac{\lambda_y^2 t}{2}\right)(\mu_y^2 - \cos^2\varphi)$$

and

$$a_1 = \frac{4}{\sqrt{\pi}} \frac{\mu_y^2}{\lambda_y^2} \sinh^2\left(\frac{\lambda_y^2 t}{2}\right).$$

The integral over $q_\perp$ can be performed analytically with the final result:

$$\Delta E_{10} = -\frac{\alpha}{\pi^{3/2}} \int_0^\infty dt\, e^{-(1-\Delta_{10})t} * \int_0^{\pi/2} d\varphi \begin{cases} \dfrac{1}{\sqrt{b_0}} \ln \dfrac{\sqrt{c}+\sqrt{b_0}}{\sqrt{c}-\sqrt{b_0}} \left(1+\dfrac{a_0}{2b_0}\right) - \dfrac{a_0\sqrt{c}}{b_0(c-b_0)} + \dfrac{\sqrt{\pi}\, a_1}{\sqrt{c}\, b_1}, & b_0 > 0, \\ \dfrac{2}{\sqrt{c}} \left(1 - \dfrac{a_0}{3c} + \dfrac{\sqrt{\pi}\, a_1}{2b_1}\right), & b_0 = 0, \\ \dfrac{2}{\sqrt{-b_0}} \arctan \sqrt{-b_0/c} \left(1+\dfrac{a_0}{2b_0}\right) - \dfrac{a_0\sqrt{c}}{b_0(c-b_0)} + \dfrac{\sqrt{\pi}\, a_1}{\sqrt{c}\, b_1}, & b_0 < 0. \end{cases} \tag{36}$$

Again, a two-dimensional integral remains.

For ΔE_{01} Eq. (36) is also valid but with a change of the values of a_0 and a_1 by

$$a_0 = \frac{4}{\lambda_z^2} \sinh^2\left(\frac{\lambda_z^2 t}{2}\right) (\mu_z^2 - \sin^2\varphi)$$

and

$$a_1 = \frac{4}{\sqrt{\pi}} \frac{\mu_z^2}{\lambda_z^2} \sinh^2\left(\frac{\lambda_z^2 t}{2}\right).$$

For the special case of the perpendicular magnetic field ($\Theta = 0°$) we obtain

$$\Delta E_{10} = -\frac{\alpha}{\pi^{1/2}} \int_0^\infty dt\, e^{-(1-\Delta_{10})t} * \begin{cases} \dfrac{1}{\sqrt{f_\eta - f_\xi}} \left[\ln \dfrac{\sqrt{f_\eta}+\sqrt{f_\eta - f_\xi}}{\sqrt{f_\xi}} \left(1 - \dfrac{h_\xi}{2(f_\eta - f_\xi)}\right) + \dfrac{h_\xi \sqrt{f_\eta}}{2f_\xi \sqrt{f_\eta - f_\xi}} \right], & \xi > \eta, \\ \dfrac{1}{\sqrt{f_\eta}} \left(1 + \dfrac{h_\xi}{3f_\xi}\right), & \xi = \eta, \\ \dfrac{1}{\sqrt{f_\xi - f_\eta}} \left[\arcsin \dfrac{\sqrt{f_\xi - f_\eta}}{\sqrt{f_\xi}} \left(1 + \dfrac{h_\xi}{2(f_\xi - f_\eta)}\right) - \dfrac{h_\xi \sqrt{f_\eta}}{2f_\xi \sqrt{f_\xi - f_\eta}} \right], & \xi < \eta, \end{cases} \tag{37}$$

with

$$h_\xi = \frac{4}{\xi}\sinh^2\frac{\xi t}{2},$$

resulting from ΔE_{10}, given in Eq. (36), if one takes the limit $\Theta \to 0°$. Here, we do not consider ΔE_{01} for the special case of a perpendicular magnetic field, because the transition $(0, 0; 0_q) \to (0, 1; 0_q)$ is not dipole-allowed for $\Theta = 0°$. For the in-plane magnetic field ($\Theta = 90°$) the result reads for $k_x = k_y = 0$,

$$\Delta E_1(0,0) = -\frac{\alpha}{\pi^{1/2}}\int_0^\infty dt\, e^{-(1-\Delta_1(0,0))t}\left\{\frac{1}{\sqrt{g_z}}\mathbf{F}(\arcsin\sqrt{g_z/t}, \gamma_z)\right.$$
$$\left.\times\left(1-\frac{h_z}{2g_z}\right)+\frac{h_z}{2g_z}\frac{\sqrt{t}}{\sqrt{(t-g_z)(t-\gamma_z^2 g_z)}}\right\} \tag{38}$$

with

$$h_z = \frac{4}{\lambda_z^2}\sinh^2\frac{\lambda_z^2 t}{2}.$$

Expanding Eqs. (37) and (38) in a power series according to ξ, we obtain the weak-magnetic field expressions for ΔE_{10} ($\Theta = 0°$) and $\Delta E_1(0, 0)$ ($\Theta = 90°$). For the difference of the energy shifts of the first excited energy level and the ground-state energy level, the weak-magnetic field expression calculated in RSPT for the special case of the perpendicular magnetic field ($\Theta = 0°$) reads

$$\Delta E_{10} - \Delta E_{00} = -\frac{\alpha}{\pi^{1/2}}\int_0^\infty dt\, e^{-t}\left\{\frac{t}{2g_\eta}\left[\frac{t}{\sqrt{g_\eta}}\arcsin\sqrt{g_\eta/t}-\sqrt{f_\eta}\right]\xi^1\right.$$
$$\left.+\frac{t^2}{8g_\eta^2}\left[\frac{3t^2}{\sqrt{g_\eta}}\arcsin\sqrt{g_\eta/t}+\sqrt{f_\eta}\,(3g_\eta+f_\eta)\right]\xi^2+\mathcal{O}(\xi^3)\right\}. \tag{39}$$

For the in-plane magnetic field ($\Theta = 90°$) the corresponding result is

$$\Delta E_1(0,0) - \Delta E_0(0,0)$$
$$= -\frac{\alpha}{\pi^{3/2}}\int_0^\infty dt\frac{e^{-t}}{\sqrt{t}}\int_0^{\pi/2} d\varphi$$
$$*\left\{\left[\frac{h_\eta}{g_\eta}\frac{1}{1-(g_\eta/t)\sin^2\varphi}-\frac{h_\eta\sqrt{t}}{2g_\eta^{3/2}\sin\varphi}\ln\frac{1+\sin\varphi\sqrt{g_\eta/t}}{1-\sin\varphi\sqrt{g_\eta/t}}\right]\xi^0\right.$$
$$\left.+\frac{1}{4\eta^2}\left[\frac{h_\eta}{g_\eta}\frac{2}{1-(g_\eta/t)\sin^2\varphi}\left(\eta t\coth\frac{\eta t}{2}-\frac{\eta t f_\eta}{g_\eta}\right.\right.\right.$$

$$+\frac{(\eta f_\eta - g_\eta/t)\sin^2\varphi + 2(g_\eta/t)\cos^2\varphi}{1-(g_\eta/t)\sin^2\varphi}\Bigg)$$

$$-\frac{h_\eta\sqrt{t}}{g_\eta^{3/2}\sin\varphi}\left(\eta t\coth\frac{\eta t}{2}-\frac{\eta t f_\eta}{g_\eta}\right)\ln\frac{1+\sin\varphi(g_\eta/t)}{1-\sin\varphi(g_\eta/t)}$$

$$-\frac{h_\eta\sqrt{t}}{2g_\eta^{3/2}\sin\varphi}*\left(\frac{\eta t f_\eta}{g_\eta}-1+2\cot^2\varphi\right)\ln\frac{1+\sin\varphi\sqrt{g_\eta/t}}{1-\sin\varphi\sqrt{g_\eta/t}}$$

$$+\frac{h_\eta}{2g_\eta}\frac{1}{1-(g_\eta/t)\sin^2\varphi}*\left(\frac{\eta t f_\eta}{g_\eta}-1+2\cot^2\varphi\right)\Bigg]\xi^2+\mathcal{O}(\xi^4)\Bigg\}. \tag{40}$$

In Figs. 2a to 2c we have plotted the EPI corrections to the levels E_{00}, E_{10}, and E_{01}, using IWBPT, with the following parameters for GaAs: $\varepsilon_\infty = 10.90$, $\varepsilon_s = 12.87$, $\hbar\omega_L = 36.17$ meV, $\alpha = 0.07$, $r_p = 3.987nm$, and $m_e = 0.06624m_0$, respectively, which are strictly valid only on the bottom of the potential of the PQW.

From Fig. 2a it is to be seen that with increasing magnetic field B and decreasing angle Θ the ground-state energy correction increases. The dependence on the strength of the magnetic field for low magnetic fields is linear for a perpendicular magnetic field, Eq. (32), but quadratic for the in-plane magnetic field, Eq. (33). The EPI correction to the energy level E_{10}, shown in Fig. 2b, goes to the same value for all tilt angles Θ for decreasing magnetic field and is identical to that of the ground state E_{00} for $B=0$. This can be seen from Eq. (39), valid for $\Theta = 0°$, where $\Delta E_{10} - \Delta E_{00}$ vanishes for $\omega_c = 0$. This is true due to the fact that the energy level $(1, 0; 0_q)$ for low magnetic fields is the first excited Landau level for all angles Θ. On the other hand, the EPI correction to the energy E_{01}, shown in Fig. 2c, goes to identically the same value for all tilt angles. But this value is different from the ground state correction ΔE_{00}. This can be seen explicitly from Eq. (40) which is valid for the case $\Theta = 90°$. Here, we have for zero magnetic field a nonvanishing difference of the corresponding EPI corrections ΔE_{01} and ΔE_{00}. This is due to the fact, that E_{01} (or E_1 for $\Theta = 90°$) is the first excited subband energy level for the vanishing magnetic field. The renormalization of different subbands due to the EPI depends on the value of the quantum number N_z.

The strong increase of the renormalization of the excited energy levels E_{10} (for $\Theta = 0°$, where the Landau levels and the subbands are independent) and E_{01} (for $\Theta > 0°$) with increasing magnetic field are due to the EPI-induced resonance coupling to the energy level $(0, 0; 1_q)$. Additionally, the anticrossing of the energy levels $(1, 0; 0_q)$ and $(0, 1; 0_q)$ for nonvanishing but small tilt angle Θ (see Figs. 2b and 2c for $\Theta = 1°$) leads to strong changes of the EPI corrections for ΔE_{10} and ΔE_{01} near the crossing point $\omega_c = \Omega$. This anticrossing effect is smeared out with increasing tilt angles (see, for instance, $\Theta = 25°$).

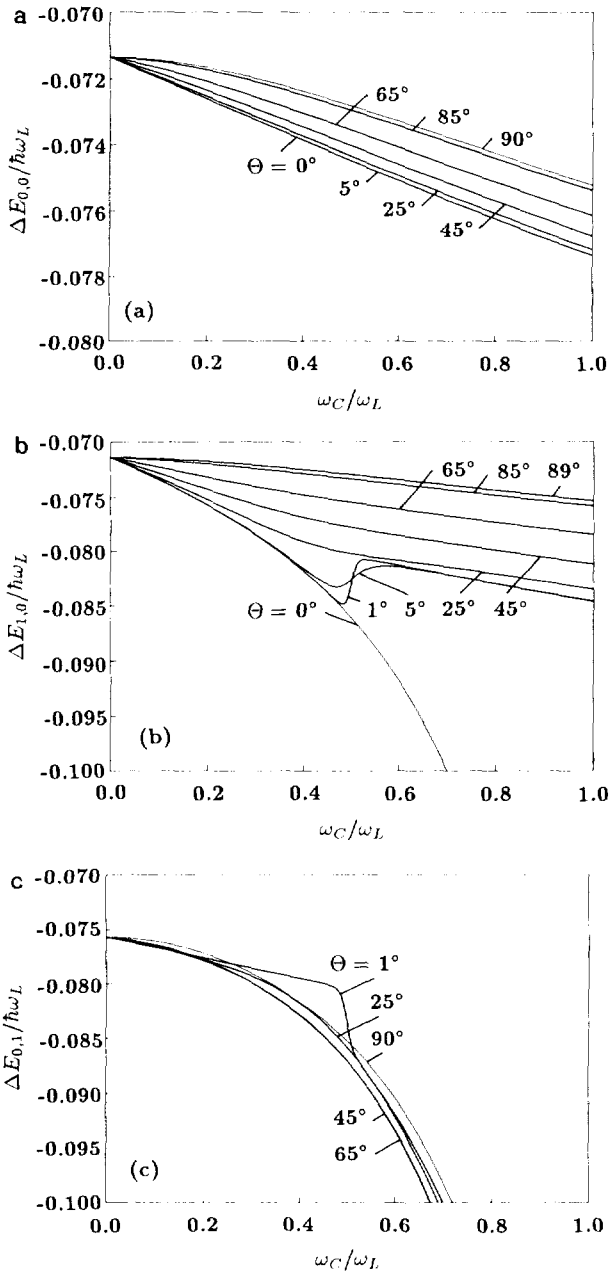

FIG. 2. The polaronic corrections $\Delta E_{00}/\hbar\omega_L$ (a), $\Delta E_{10}/\hbar\omega_L$ (b), and $\Delta E_{01}/\hbar\omega_L$ (c) as a function of the magnetic field in a PQW with a confinement frequency of $\Omega/\omega_L = 0.5$ for different angles Θ. The thin solid lines correspond to the special cases of perpendicular ($\Theta = 0°$) and in-plane ($\Theta = 90°$) magnetic fields.

In Figs. 3a to 3e the calculated magnetopolaron levels are plotted. The thin solid lines show the unperturbed levels $(N_y, N_z; 0_q)$, the thin dashed line the unperturbed level $(0, 0; 1_q)$, and the heavy solid lines are the corresponding magnetopolaron levels, including the EPI. The magnetopolaron levels are calculated from Eqs. (28) and (36). For vanishing tilt angle Θ only the Landau level $(1, 0; 0_q)$ is excitable by FIR radiation, but not the subband level $(0, 1; 0_q)$. Therefore for a perpendicular magnetic field $(\Theta = 0°)$ only the two magnetopolaron levels $(0, 0; 0_q)$ and $(1, 0; 0_q)$ are shown in Fig. 3a. Resonance of the excited level $(1, 0; 0_q)$ with the one-LO phonon level $(0, 0; 1_q)$ occurs at $\omega_c^R = \omega_L$. This EPI-induced resonance leads to a splitting of the excited level $(1, 0; 0_q)$ and the level $(0, 0; 1_q)$ at the resonance point $\omega_c^R = \omega_L$. This second type of resonant level splitting, caused by EPI, is called resonant magnetopolaron level coupling (RMPLC). In Fig. 3 only the lower energetic branch of the two split energy levels $(E_{10} \to E_{10}^{\pm})$ is calculated. The higher energetic branch E_{10}^{+} is not calculated here, because the condition $D_{N_z' N_z}^{N_y' N_y} > 0$ restricts the calculations to energies below $\hbar\omega_L + \hbar\omega_y/2 + \hbar\omega_z/2 + \Delta E_{00}^{\mathrm{RSPT}}$ in IWBPT. It is well known that in 3D semiconductors the upper branch is located in the phonon continuum which has a threshold energy $E_{th} = \hbar\omega_L + \hbar\omega_c/2 + \Delta E_0^{\mathrm{RSPT}}$. In the here considered case we have for $\Theta \neq 90°$ a complete quantized state and, hence, there is no phonon continuum. But for $\Theta = 90°$ a phonon continuum exists with the threshold energy $E_{th} = \hbar\omega_L + \hbar\tilde{\omega}_c/2 + \Delta E_0^{\mathrm{RSPT}}(0, 0)$. Hence, if one wants to calculate the upper branch and the splitting of the two branches $E_{10}^{\pm}$ at the resonance it is necessary to calculate Eq. (23) without using Eq. (25). One possibility for this calculation is the so-called resonance approximation. This means that one includes in the calculation of the energy shifts ΔE_{10} at the resonance only the main contributing term of the sum in Eq. (23) which is the term with $N_y' = N_z' = 0$ [56]. Hence, for example, in the case $\Theta = 0°$ we have

$$\Delta E_{10} = -\frac{f_{\substack{01\\00}}^{\mathrm{LO}}}{\hbar(\omega_L - \omega_c) - \Delta_{10}}\bigg|_{\omega_c = \omega_L} \tag{41}$$

with

$$f_{\substack{01\\00}}^{\mathrm{LO}} = \sum_{\mathbf{q}} |M_{00}^{01}(\mathbf{q})|^2$$

$$= \frac{\alpha}{2\sqrt{\pi}} \begin{cases} \dfrac{\sqrt{\eta}}{1-\eta}\left(1 - \dfrac{\eta}{\sqrt{1-\eta}} \ln \dfrac{1-\sqrt{1-\eta}}{\sqrt{\eta}}\right), & 0 < \eta < 1, \\ \dfrac{2}{3}, & \eta = 1, \\ \left(\dfrac{\eta}{\eta-1}\right)^{3/2} (\arcsin\sqrt{(\eta-1)/\eta} - \sqrt{(\eta-1)/\eta}), & \eta > 1. \end{cases} \tag{42}$$

The energy shift ΔE_{10} at the resonance results in a splitting of the level E_{10} into the levels $E_{10}^{\pm} = \mathscr{E}_{10} + \Delta E_{10}^{\pm}$, according to

$$\Delta E_{10}^{\pm} = \begin{cases} -\Delta E_{00}/2 \pm \sqrt{f_{\substack{01\\00}}^{\mathrm{LO}} + \Delta E_{00}^2/4}, & \text{IWBPT}, \\ \pm\sqrt{f_{\substack{01\\00}}^{\mathrm{LO}}}, & \text{WBPT}, \end{cases} \tag{43}$$

and following the splitting $\delta_{10} = \Delta E_{10}^{+} - \Delta E_{10}^{-}$ is

$$\delta_{10} = \alpha^{1/2} \sqrt{2/\sqrt{\pi}} \begin{cases} \sqrt{\dfrac{\sqrt{\eta}}{1-\eta}\left(1 - \dfrac{\eta}{\sqrt{1-\eta}} \ln \dfrac{1-\sqrt{1-\eta}}{\sqrt{\eta}}\right)}, & 0 < \eta < 1, \\ \sqrt{2/3}, & \eta = 1, \\ \sqrt{\left(\dfrac{\eta}{\eta-1}\right)^{3/2}\left(\arcsin\sqrt{\dfrac{\eta-1}{\eta}} - \dfrac{\sqrt{\eta-1}}{\eta}\right)}, & \eta > 1, \end{cases} \tag{44}$$

if we use WBPT. Hence, the splitting is $\propto \alpha^{1/2}$, which is the same proportionality as for the 2D resonant magnetopolaron [25] as opposed to the $\alpha^{2/3}$ dependence of a 3D resonant magnetopolaron [55]. For an infinitesimally thin PQW

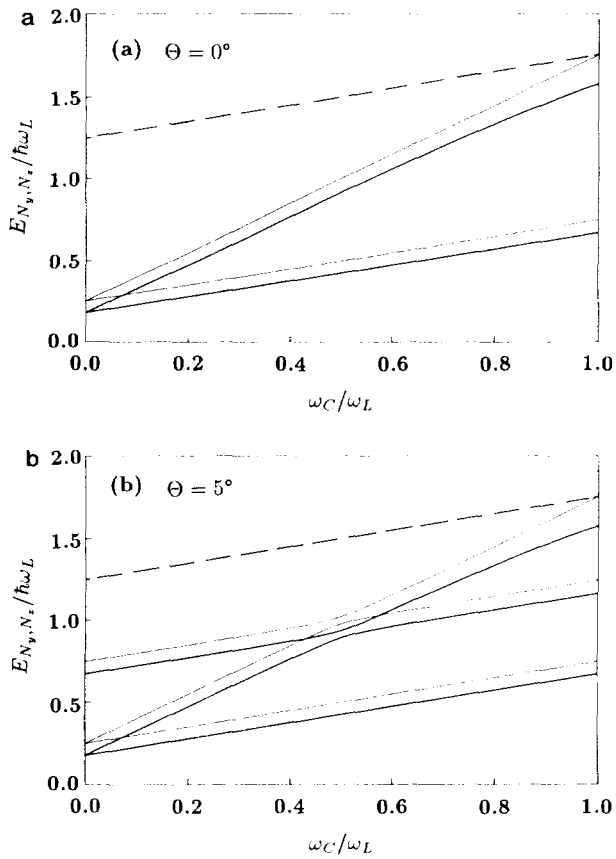

FIG. 3. The first magnetopolaron levels E_{00}, E_{10}, and E_{01} (thick solid lines) as a function of the magnetic field in a PQW for $\Omega/\omega_L = 0.5$ and different angles Θ. The corresponding unperturbed energy levels are plotted by thin solid $(0, 0; 0_q)$, $(1, 0; 0_q)$, $(0, 1; 0_q)$ and dashed $(0, 0; 1_q)$ lines.

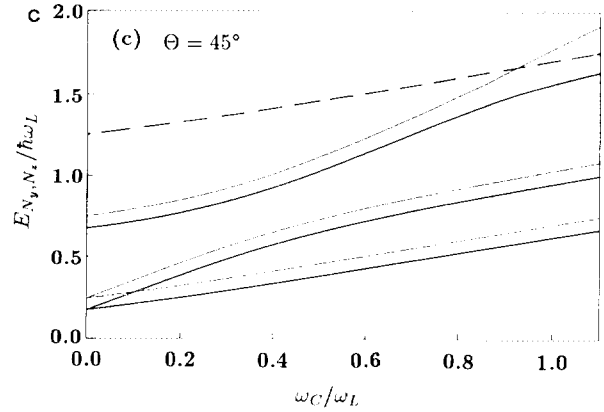

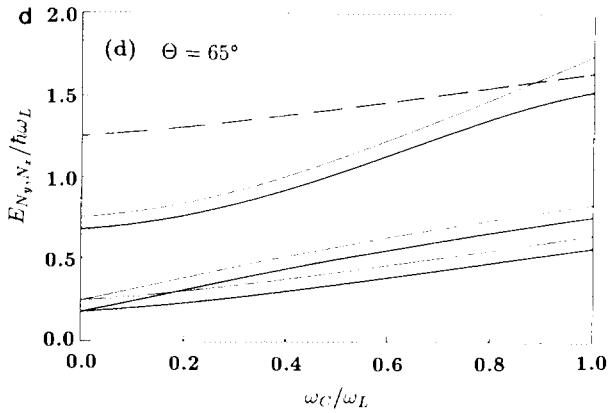

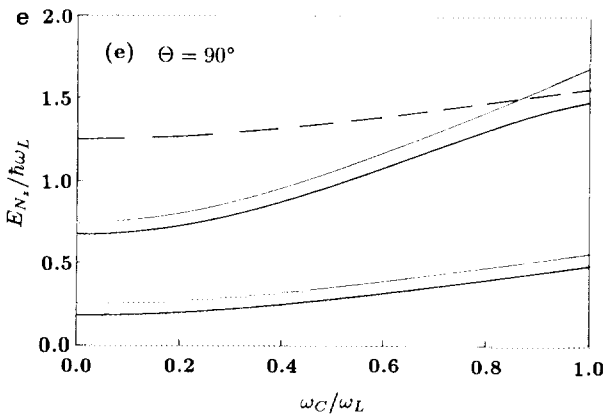

FIG. 3—*Continued.*

($\eta = \Omega/\omega_L \to \infty$) we obtain the limit of the strict 2D resonant magnetopolaron [25] for which the splitting is equal to $\delta_{10} = (\pi^{1/2}\alpha)^{1/2}$. This result can be extended [57] to the case of a tilted magnetic field ($0° < \Theta < 90°$).

If one applies a weakly tilted magnetic field (see Fig. 3b, $\Theta = 5°$), additionally the energy level $(0, 1; 0_q)$ can be excited by cyclotron resonance. Because of the anticrossing of the pure electron levels at $\omega_c = \Omega$ the magnetopolaron levels $(1, 0; 0_q)$ and $(0, 1; 0_q)$ change their character for small magnetic fields ($\omega_c < \Omega$) from Landau-like and subband-like for high magnetic fields ($\omega_c > \Omega$) to subband-like and Landau-like levels. Therefore, the level $(0, 1; 0_q)$ is resonant with the LO phonon for a cyclotron frequency $\omega_c^R = \omega_L(\omega_L^2 - \Omega^2)^{1/2}/(\omega_L^2 - \Omega^2 \cos^2 \Theta)^{1/2}$ which is a little bit lower than in the case $\Theta = 0°$ ($\omega_c^R = \omega_L$). This resonance decreases for increasing tilt angle Θ. For the in-plane magnetic field $\Theta = 90°$ (Fig. 3e) only the mixed subband-Landau level $(1, 0, 0; 0_q)$ is exitable by cyclotron resonance. In this

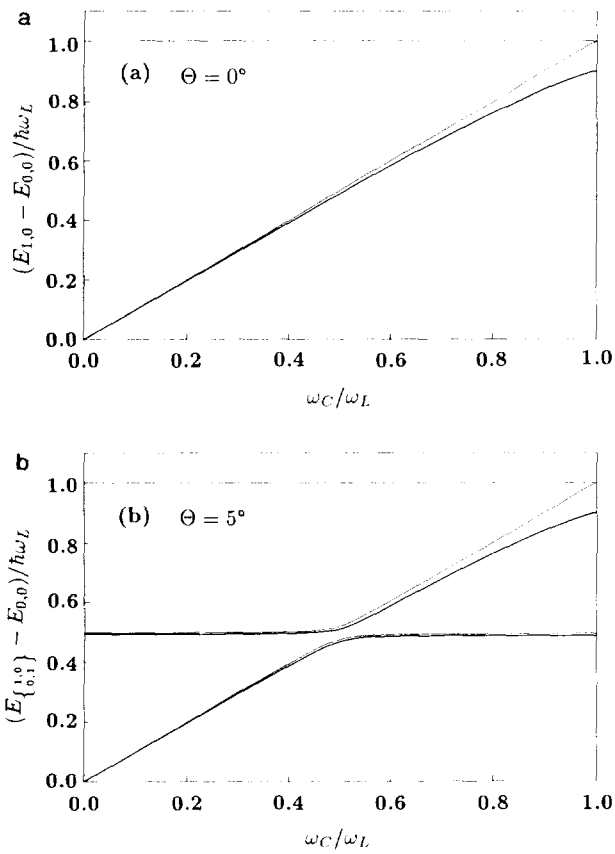

FIG. 4. Energy difference between the energy levels $E_{10} - E_{00}$ and $E_{01} - E_{00}$ for the perturbed states (magnetopolaron, thick solid lines) and the unperturbed states (electron, thin solid lines) for a PQW for $\Omega/\omega_L = 0.5$ and different angles Θ.

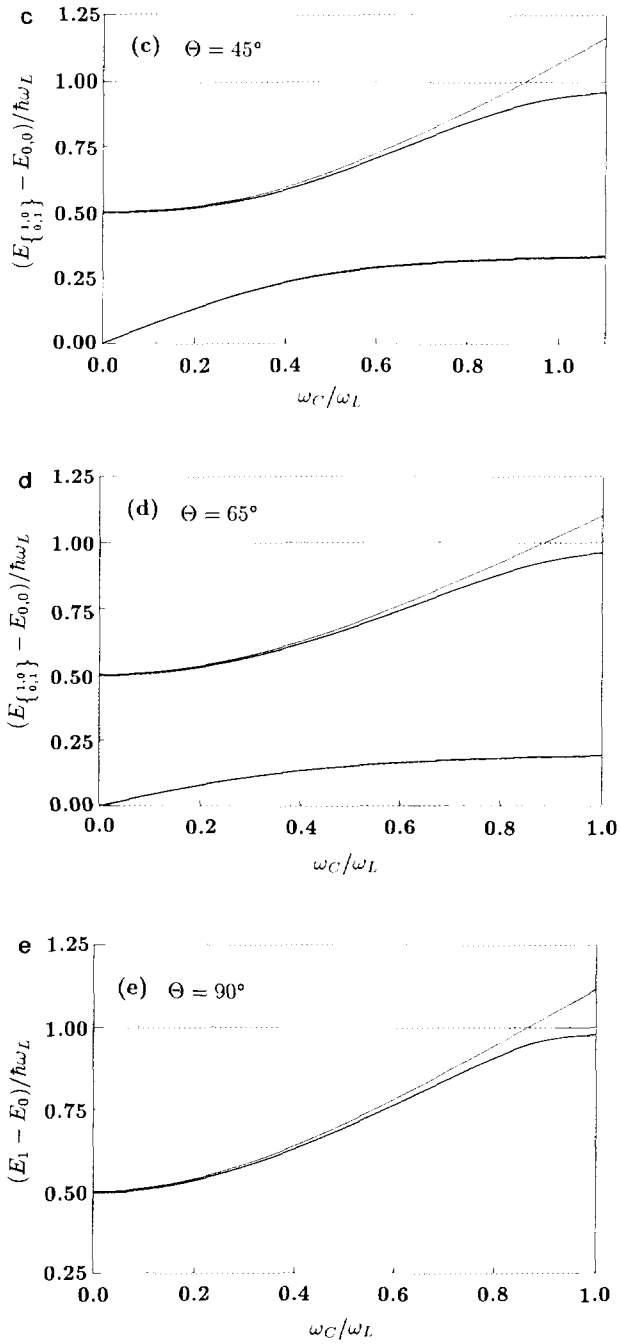

FIG. 4—*Continued.*

case resonance occurs for the cyclotron frequency equal to $\omega_c^R = \sqrt{\omega_L^2 - \Omega^2}$, which is equal to the resonance frequency in the case of a parabolic QWW [47].

In cyclotron resonance experiments the transitions of electrons between the energy levels, which are in polar semiconductors magnetopolaron levels, are observed. Hence, the transitions between the plotted magnetopolaron levels of Figs. 3 are detected. The energy differences $E_{10} - E_{00}$ and $E_{01} - E_{00}$ are plotted in Figs. 4a to 4e. The heavy solid lines represent the renormalized energy difference and the thin solid lines are those of the unperturbed levels. Figures 4a–e show that the transition energies measured in cyclotron resonance experiments are reduced due to the EPI, especially for increasing magnetic fields. Near the resonance to the LO phonon the transition energy is pinned below the LO phonon energy $\hbar\omega_L$. This resonance, occuring at $\Theta = 0°$ (Fig. 4a) for the transition $(0, 0; 0_q) \to (1, 0; 0_q)$, changes at $\Theta > 0°$ (Figs. 4b–e) to the transition $(0, 0; 0_q) \to (0, 1; 0_q)$ due to the anticrossing of the levels $(1, 0; 0_q)$ and $(0, 1; 0_q)$ which is seen from Fig. 3. Note that for weak magnetic fields the level $(0, 1; 0_q)$ is a subband-like energy level. Different subband levels are differently renormalized by the EPI. This can be seen explicitly from Eq. (40) for the special case of the in-plane magnetic field, where the difference of the energy renormalization $\Delta E_1 - \Delta E_0$ remains finite for the vanishing magnetic field. The frequency of the transition $(0, 0; 0_q) \to (0, 1; 0_q)$ is decreased already for vanishing magnetic fields, contrary to the other transition. According to the smallness of this difference ($\approx 0.004 * \omega_L$) this effect cannot be drawn in Figs. 4b–e.

IV. Polaron Cyclotron Mass

In the cyclotron resonance experiment the optical transitions $E_{00} \to E_{10}$ and $E_{00} \to E_{01}$ can be used to determine the cyclotron mass m_c^*. From Figs. 1a and 3a it can be seen that for $\Theta = 0°$ only the transition $E_{00} \to E_{10}$ yields the resonant magnetopolaron case at $\omega_c^R = \omega_L$ ($B = B_L$). In the general case of tilted magnetic field for $\Theta \neq 0°$ the situation is changed (see Figs. 1b to 1f and 3b to 3d). Because of the anticrossing of the levels E_{10} and E_{01} at $\omega_c = \Omega$ due to RSLC, now the transition $E_{00} \to E_{01}$ yields the resonant magnetopolaron case. For the in-plane magnetic field the corresponding transition $E_0(0, 0) \to E_1(0, 0)$ yields the resonant magnetopolaron (Figs. 1g and 3e). If one neglects for the moment the EPI the transition $\mathscr{E}_{00} \to \mathscr{E}_{10}$ is detected at the transition frequency $\omega_y = (\mathscr{E}_{10} - \mathscr{E}_{00})/\hbar$ which is connected to the cyclotron frequency $\omega_c = [2\omega_y^2(\omega_y^2 - \Omega^2)/(2\omega_y^2 - \Omega^2(1 + \cos 2\Theta))]^{1/2}$ according to Eq. (7). Including the EPI the transition frequency ω_y and the cyclotron frequency ω_c is renormalized to ω_y^* and ω_c^{10*}. Hence, the polaron cyclotron mass $m_c^{10*} = eB/\omega_c^{10*}$ is given by

$$\frac{m_c^{10*}}{m_e} = \frac{\sqrt{2\left(\frac{1}{\gamma_y} + \frac{\Delta E_{10} - \Delta E_{00}}{\xi}\right)^2 - \left(\frac{\eta}{\xi}\right)^2 (1 + \cos(2\Theta))}}{\sqrt{2}\left(\frac{1}{\gamma_y} + \frac{\Delta E_{10} - \Delta E_{00}}{\xi}\right)\sqrt{\left(\frac{1}{\gamma_y} + \frac{\Delta E_{10} - \Delta E_{00}}{\xi}\right)^2 - \left(\frac{\eta}{\xi}\right)^2}}. \tag{45}$$

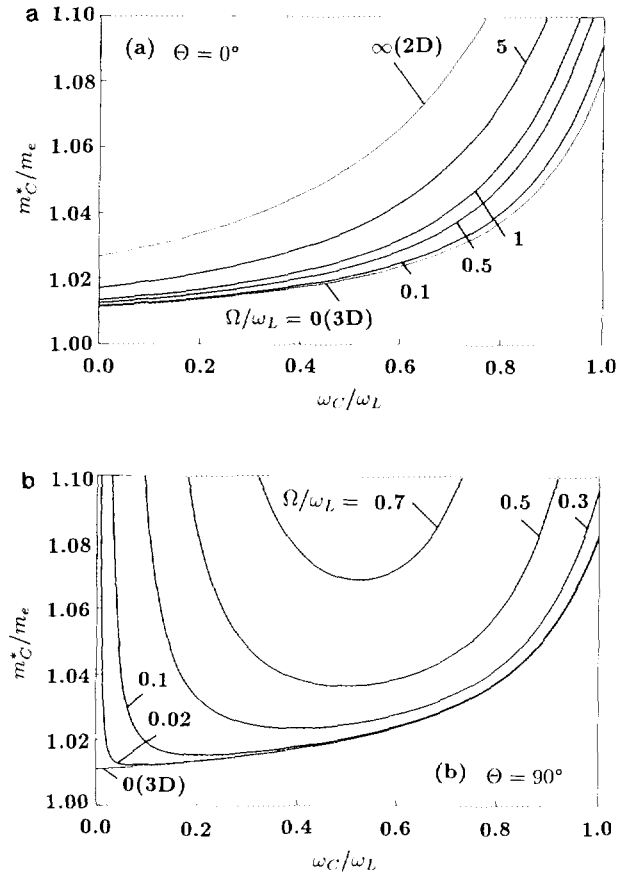

FIG. 5. Polaron cyclotron mass of the Q2D magnetopolaron versus magnetic field in a PQW for a perpendicular ($\Theta = 0°$) magnetic field and different confinement frequencies Ω (a): the thin solid lines correspond to the special case of zero confinement frequency, i.e., 3D magnetopolaron; and of infinite confinement frequency, i.e., 2D magnetopolaron and for an in-plane ($\Theta = 90°$) magnetic field and different confinement frequencies Ω (b): the thin solid line corresponds to the special case of zero confinement frequency, i.e., the 3D magnetopolaron.

In a similar way the corresponding polaron cyclotron mass $m_c^{01*} = eB/\omega_c^{01*}$ for the transition $E_{00} \to E_{01}$ is calculated to be

$$\frac{m_c^{01*}}{m_e} = \frac{\sqrt{2\left(\frac{1}{\gamma_z} + \frac{\Delta E_{01} - \Delta E_{00}}{\xi}\right)^2 - \left(\frac{\eta}{\xi}\right)^2 (1 + \cos(2\Theta))}}{\sqrt{2}\left(\frac{1}{\gamma_z} + \frac{\Delta E_{01} - \Delta E_{00}}{\xi}\right)\sqrt{\left(\frac{1}{\gamma_z} + \frac{\Delta E_{01} - \Delta E_{00}}{\xi}\right)^2 - \left(\frac{\eta}{\xi}\right)^2}}. \tag{46}$$

with $\omega_c^{01*} = [2\omega_z^{*2}(\omega_z^{*2} - \Omega^2)/(2\omega_z^{*2} - \Omega^2(1 + \cos 2\Theta))]^{1/2}$ and $\omega_z^* = (E_{01} - E_{00})/\hbar$. For the case of the perpendicular magnetic field ($\Theta = 0°$) the transition $E_{00} \to E_{10}$ yields the polaron cyclotron mass defined by

$$\frac{m_c^*}{m_e} = 1 \Big/ \left(1 + \frac{\Delta E_{10} - \Delta E_{00}}{\xi}\right) \tag{47}$$

which is equal to the usual polaron cyclotron mass definition for 2D and 3D magnetopolarons. For the second special case, the in-plane magnetic field ($\Theta = 90°$), the transition $E_0(0, 0) \to E_1(0, 0)$ defines the polaron cyclotron mass:

$$\frac{m_c^*}{m_e} = 1 \Big/ \sqrt{1 + \left(\frac{\Delta E_1 - \Delta E_0}{\xi}\right)^2 + 2\,\frac{\Delta E_1 - \Delta E_0}{\gamma_z \xi}}. \tag{48}$$

The polaron cyclotron mass is shown in Figs. 5 and 6. The special case of the perpendicular magnetic field ($\Theta = 0°$) is plotted in Fig. 5a for different values of the confinement energy $\hbar\Omega$, using Eq. (47) for the case of the IWBPT. It is seen that with increasing magnetic field the polaron cyclotron mass increases. This is a result of the polaron induced nonparabolicity of the energy dispersion in absence of the conduction band nonparabolicity. The strong enhancement of the polaron cyclotron mass near the unperturbed level crossing at $\omega_c^R = \omega_L$ is a consequence of the pinning of the level E_{10} to the energy $\hbar\omega_L + \hbar\omega_c/2 + \hbar\Omega/2 + \Delta E_{00}^{\mathrm{RSPT}}$. For the case of a perpendicular magnetic field and in the weak-magnetic field limit $\xi = \omega_c/\omega_L \ll 1$, the expansion of the polaron cyclotron mass m_c^* (Eq. (47)), in a power series according to ξ, gives the result

$$\frac{m_c^*}{m_e} = \left[1 - \alpha\,\frac{1}{\pi^{1/2}} \int_0^\infty dt\, e^{-t} \left\{ \frac{t}{2g_\eta} \left[\frac{t}{\sqrt{g_\eta}} \arcsin \sqrt{g_\eta/t} - \sqrt{f_\eta} \right] \xi^0 \right.\right.$$
$$\left.\left. + \frac{t^2}{8g_\eta^2} \left[\frac{3t^2}{\sqrt{g_\eta}} \arcsin \sqrt{g_\eta/t} + \sqrt{f_\eta}\,(3g_\eta + f_\eta) \right] \xi^1 + \mathcal{O}(\xi^2) \right\} \right]^{-1}. \tag{49}$$

For vanishing confinement $\Omega = 0$ one describes the polaron cyclotron mass of a 3D magnetopolaron. This is obtained explicitly from Eq. (49):

$$\frac{m_c^*}{m_e} = 1 \Big/ \left(1 - \frac{\alpha}{6}\left(1 + \frac{9}{10}\,\xi + \mathcal{O}(\xi^2)\right)\right). \tag{50}$$

In the case of a vanishing magnetic field this expression includes the special case of the polaron mass $m^*/m_e = [1 - \alpha/6]^{-1}$ of a 3D polaron [25]. But for $\Omega \to \infty$, the confining potential is infinitesimal thin and, therefore, we obtain the well-known polaron cyclotron mass of a 2D magnetopolaron. In this case, Eq. (49) reads

$$\frac{m_c^*}{m_e} = 1 \Big/ \left(1 - \frac{\pi}{8}\,\alpha\left(1 + \frac{9}{8}\,\xi + \mathcal{O}(\xi^2)\right)\right). \tag{51}$$

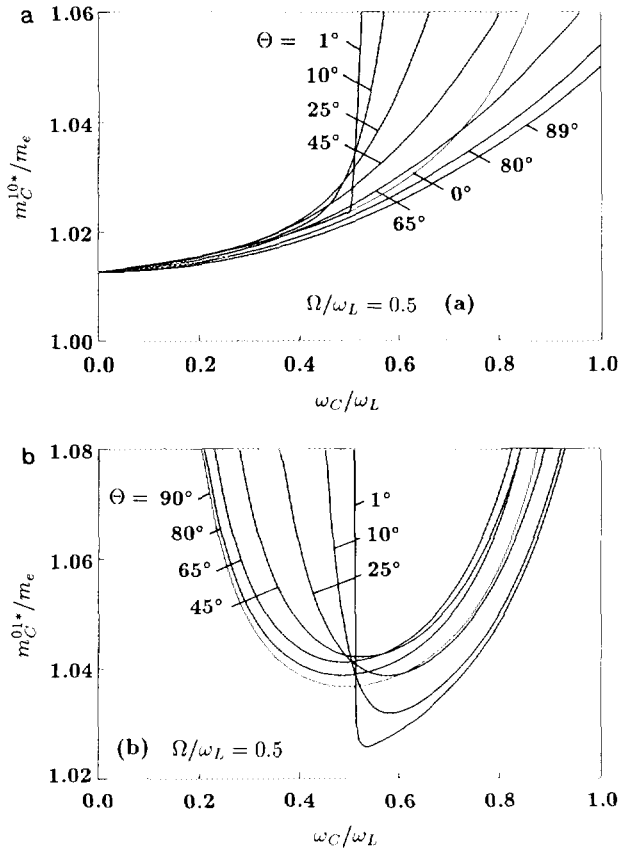

FIG. 6. Polaron cyclotron mass of the Q2D magnetopolaron versus magnetic field in a PQW for a confinement frequency $\Omega/\omega_L = 0.5$ and for different angles Θ (a) m_c^{10*}; (b) m_c^{01*}; the thin solid lines correspond to the special cases of in-plane and perpendicular magnetic field.

For a vanishing magnetic field, Eq. (47) gives the well-known polaron mass $m^*/m_e = [1 - \alpha\pi/8]^{-1}$ of the 2D polaron [25].

In Fig. 5b the polaron cyclotron mass is plotted for the case of an in-plane magnetic field ($\Theta = 90°$) for different values of the confinement energy $\hbar\Omega$ calculated using Eq. (48). For small magnetic fields ($B \to 0$) this mass increases with decreasing magnetic field. In this case the quantization of the electrons motion in z-direction arises from size- and magnetic-quantization. For $B \to 0$ the quantum confinement in z-direction of the structure results more and more from the quantum-size effect of the parabolic potential. In this case the polaron corrections to the energy levels are different for all levels including the case of vanishing magnetic field. For a vanishing magnetic field the electron is purely confined due to the parabolic potential. Therefore no mass connected with kinetic energy motion in this direction exists. For $\Theta = 90°$ the denominator of Eq. (48) has a zero for a certain

magnetic field, which depends on the geometrical confinement frequency Ω. Only for larger magnetic fields as this above-defined critical one, is it possible to determine the polaron cyclotron mass by a cyclotron resonance experiment. This physical behaviour of m_c^* for $\Theta = 90°$ is very similar to the case of Q1D magnetopolarons in QWW's [47].

If one tilts the angle Θ of the magnetic field with respect to the z-axis one obtains two branches, m_c^{10*} and m_c^{01*}, of the polaron cyclotron mass. These two branches are plotted in Figs. 6a and 6b for different tilt angles Θ. Due to the anticrossing of the excited magnetopolaron levels for small tilt angles $\Theta > 0°$ at $\omega_c \approx [2\omega_y^2(\omega_y^2 - \Omega^2)/(2\omega_y^2 - \Omega^2(1 + \cos 2\Theta))]^{1/2}$ we obtain a drastic increase of the polaron cyclotron mass m_c^{10*} (Fig. 5c) for $\omega_c > [2\omega_y^2(\omega_y^2 - \Omega^2)/(2\omega_y^2 - \Omega^2(1 + \cos 2\Theta))]^{1/2}$. With increasing tilt angle Θ there is a decrease of the polaron cyclotron mass m_c^{10*} especially for high magnetic fields due to the absence of the resonance with the LO phonon of this excited level $(1, 0; 0_q)$ for tilt angles $\Theta > 0°$ (cf. Figs. 3b–e). The polaron cyclotron mass m_c^{01*} shows the typical resonance enhancement near $\omega_c = [2\omega_y^2(\omega_y^2 - \Omega^2)/(2\omega_y^2 - \Omega^2(1 + \cos 2\Theta))]^{1/2}$ which is shifted to lower values with increasing tilt angle Θ according to the Θ-dependence of this resonance point. The divergency of the polaron cyclotron mass for lower magnetic fields according to the subband-like character of the considered transition is also shifted to lower magnetic fields with increasing tilt angle Θ and reaches the limit for the in-plane magnetic field (Fig. 5b) for $\Theta = 90°$.

V. Summary

We have calculated the polaron corrections to the electron energy levels and the cyclotron mass of magnetopolarons confined in a PQW in a tilted magnetic field. Our results are valid for zero temperature and arbitrary magnetic field strength. It is shown that in a tilted magnetic field the one-electron levels split at $\omega_c = \Omega$ due to the RSLC. A further level splitting arises from polaronic effects as a result of the RMPLC. Without EPI the energy levels $(N_y, N_z; 0_q)$ can cross the level $(0, 0; 1_q)$. But the EPI causes a resonance splitting and, therefore, the degeneracy is lifted. Whereas this resonance always occurs for $\Theta \neq 90°$, for the in-plane magnetic field case $(\Theta = 90°)$ it depends on the ratio of the confinement energy and the LO phonon energy if this resonance occurs or not. The case of an in-plane magnetic field plays a special role. This case shows some similarities with magnetopolarons in quasi-one-dimensional QWW's [47]. For $\Theta \neq 90°$ the energy spectrum is entirely discrete and the levels are macroscopic degenerated according to the electron momentum $\hbar k_x$. But for the case $\Theta = 90°$ anisotropic quasi-two-dimensional subbands arise and the degeneracy is lifted. We have shown that for $\Theta \neq 90°$ the polaronic level splitting is $\propto \alpha^{1/2}$ in the resonance approximation which is the same dependence as for 2D magnetopolarons in a perpendicular magnetic field. The here obtained results, based on a one-polaron theory, are valid for perfect parabolic potentials built up from semiconductor materials with a parabolic conduction band.

To improve on these results one has to include in the calculation a possible nonparabolicity of the conduction band (band structure effect), the nonparabolicity of the confining potential and, if many electrons are present, occupation and screening effects. It is well known [14] that in the absence of the electron–phonon interaction in a cyclotron resonance experiment the PQW absorbes FIR radiation only at two frequencies, independent of the number of electrons in the well, and also independent of the electron–electron interaction. This result, the so-called generalized Kohn's theorem will be violated by the EPI developed in this paper.

REFERENCES

1. B. I. HALPERIN, *Jpn J. Appl. Phys. Suppl.* **26**, No. 3 (1987), 1913.
2. M. SHAYEGAN, T. SAJOTO, M. SANTOS, AND C. SILVESTRE, *Appl. Phys. Lett.* **53** (1988), 791.
3. E. G. GWINN, R. M. WESTERVELT, P. F. HOPKINS, A. J. RIMBERG, M. SUNDARAM, AND A. C. GOSSARD, *Phys. Rev. B* **39** (1989), 6260.
4. K. ENSSLIN, M. SUNDARAM, A. WIXFORTH, J. H. ENGLISH, AND A. C. GOSSARD, *Phys. Rev. B* **43** (1991), 9988; K. ENSSLIN, C. PISTITSCH, A. WIXFORTH, M. SUNDARAM, P. F. HOPKINS, AND A. C. GOSSARD, *Phys. Rev. B* **45** (1992), 11,407.
5. K. KARRAÏ, H. D. DREW, M. W. LEE, AND M. SHAYEGAN, *Phys. Rev. B* **39** (1989), 1426; K. KARRAÏ, X. YING, H. D. DREW, AND M. SHAYEGAN, *Phys. Rev. B* **40** (1989), 12,020.
6. X. YING, K. KARRAÏ, H. D. DREW, M. SANTOS, AND M. SHAYEGAN, *Phys. Rev. B* **46** (1992), 1823.
7. A. WIXFORTH, M. SUNDARAM, J. H. ENGLISH, AND A. C. GOSSARD, *in* "Proceedings, 20th International Conference on the Physics of Semiconductors" (M. Anastassakis and J. D. Joannopoulos, Eds.), p. 1705, World Scientific, Singapore, 1990.
8. A. WIXFORTH, M. SUNDARAM, K. ENSSLIN, J. H. ENGLISH, AND A. C. GOSSARD, *Phys. Rev. B* **43** (1991), 10,000.
9. J. H. BURNETT, H. M. CHENG, W. PAUL, P. F. HOPKINS, E. G. GWINN, A. J. RIMBERG, R. M. WESTERVELT, M. SUNDARAM, AND A. C. GOSSARD, *Phys. Rev. B* **43** (1991), 12,033.
10. V. CELLI AND D. N. MERMIN, *Phys. Rev.* **140** (1965), A839.
11. Z. TESANOVICH AND B. I. HALPERIN, *Phys. Rev. B* **36** (1987), 4888.
12. A. H. MACDONALD AND G. W. BRYANT, *Phys. Rev. Lett.* **58** (1987), 515.
13. P. RUDEN AND G. H. DÖHLER, *Phys. Rev. B* **27** (1983), 3547.
14. L. BREY, N. F. JOHNSON, AND B. I. HALPERIN, *Phys. Rev. B* **40** (1989), 10,647.
15. L. BREY, J. DEMPSEY, N. F. JOHNSON, AND B. I. HALPERIN, *Phys. Rev. B* **42** (1990), 1240.
16. L. BREY, N. F. JOHNSON, AND J. DEMPSEY, *Phys. Rev. B* **42** (1990), 2886.
17. J. DEMPSEY AND B. I. HALPERIN, *Phys. Rev. B* **45** (1992), 3902.
18. C. KUPER AND G. WHITFIELD (Eds.), "Polarons and Excitons," Oliver & Boyd, Edinburgh, 1963.
19. J. T. DEVREESE (Ed.), "Polarons in Ionic Crystals and Polar Semiconductors," North-Holland, Amsterdam, 1972.
20. D. M. LARSEN, *in* "Polarons in Ionic Crystals and Polar Semiconductors" (J. T. Devreese, Ed.), p. 237, North-Holland, Amsterdam, 1972.
21. G. LINDEMANN, R. LASSNIG, W. SEIDENBUSCH, AND E. GORNIK, *Phys. Rev. B* **28** (1983), 4693.
22. H. SIGG, H. J. A. BLUYSSEN, AND P. WYDER, *Solid State Commun.* **48** (1983), 897.
23. D. M. LARSEN, *Phys. Rev.* **135** (1964), A419; **180** (1969), 919.
24. F. M. PEETERS AND J. T. DEVREESE, *Physica B* **127** (1984), 408.
25. F. M. PEETERS AND J. T. DEVREESE, *Phys. Rev. B* **31** (1985), 3689.
26. S. DAS SARMA AND A. MADHUKAR, *Phys. Rev. B* **22** (1980), 2823.
27. D. LARSEN, *Phys. Rev. B* **30** (1984), 4595.
28. S. DAS SARMA, *Phys. Rev. Lett.* **52** (1984), 859.
29. W. SEIDENBUSCH, G. LINDEMANN, R. LASSNIG, J. EDLINGER, AND E. GORNIK, *Surf. Sci.* **142** (1984), 375.

30. M. HORST, U. MERKT, W. ZAWADZKI, J. C. MAAN, AND K. PLOOG, *Solid State Commun.* **53** (1985), 403.
31. H. SIGG, P. WYDER, AND J. A. A. J. PERENBOOM, *Phys. Rev. B* **31** (1985), 5253.
32. M. A. HOPKINS, R. J. NICHOLAS, M. A. BRUMMELL, J. J. HARRIS, AND C. T. B. FOXON, *Superlattices Microstruct.* **2** (1986), 319; *Phys. Rev. B* **36** (1987), 4789.
33. M. HORST, U. MERKT, AND J. P. KOTTHAUS, *Phys. Rev. Lett.* **50** (1983), 754.
34. U. MERKT, M. HORST, AND J. P. KOTTHAUS, *Phys. Scripta T* **13** (1986), 272.
35. M. ZIESMANN, D. HEITMANN, AND L. L. CHANG, *Phys. Rev. B* **35** (1987), 4541.
36. J. SINGLETON, R. J. NICHOLAS, D. C. ROGERS, AND C. T. B. FOXON, *Surf. Sci.* **196** (1988), 429.
37. J. SINGLETON, R. J. NICHOLAS, AND F. NASIR, *Solid State Commun.* **58** (1986), 833.
38. R. LASSNIG AND W. ZAWADZKI, *Surf. Sci.* **142** (1984), 388.
39. X. WU, F. M. PEETERS, AND J. T. DEVREESE, *Phys. Rev. B* **34** (1986), 8800; **40** (1989), 4090.
40. F. A. P. OSÓRIO, M. H. DEGANI, AND O. HIPÓLITO. *Phys. Rev. B* **38** (1988), 8477.
41. X. WU, F. M. PEETERS, AND J. T. DEVREESE, *Phys. Rev. B* **36** (1987), 9760.
42. F. M. PEETERS, X. WU, AND J. T. DEVREESE, *Surf. Sci.* **196** (1988), 437.
43. W. MÜLLER, H. T. GRAHN, R. J. HAUG, AND K. PLOOG, *Phys. Rev. B* **46** (1992), 9800.
44. L. WENDLER, *Phys. Status Solidi B* **129** (1985), 513.
45. G. Q. HAI, F. M. PEETERS, AND J. T. DEVREESE, *in* "Proceedings, NATO Advanced Research Workshop on Phonons in Semiconductor Nanostructures, St-Feliu de Guixols, 1992."
46. U. MERKT, *Phys. Scripta T* **23** (1988), 63.
47. L. WENDLER, A. V. CHAPLIK, R. HAUPT, AND O. HIPÓLITO, *J. Phys.: Condens. Matter* **5** (1993), 4817.
48. L. WENDLER, A. V. CHAPLIK, R. HAUPT, AND O. HIPÓLITO, *J. Phys.: Condens. Matter* **5** (1993), 8031.
49. J. C. MAAN, *in* "Two-Dimensional Systems, Heterostructures and Superlattices" (G. Bauer, F. Kuchar, and H. Heinrich, Eds.), Vol.53, "Solid State Sciences," Springer-Verlag, Berlin, 1984.
50. R. MERLIN, *Solid State Commun.* **64** (1987), 99.
51. U. MERKT, *in* "Festkörperprobleme" (P. Grosse, Ed.), Vol. 27, p. 109, "Advances in Solid State Physics," Vieweg, Braunschweig, 1987.
52. H. FRÖHLICH, *Adv. Phys.* **3** (1954), 325.
53. L. WENDLER AND R. HAUPT, *Phys. Status Solidi B* **143** (1987), 487.
54. R. HAUPT AND L. WENDLER, *Phys. Rev. B* **44** (1991), 1850.
55. I. B. LEVINSON AND E. I. RASHBA, *Usp. Fiz. Nauk* **111** (1973), 683 (*Sov. Phys. Usp.* **16** (1974), 892).
56. R. HAUPT AND L. WENDLER, *Solid State Commun.* **89** (1994), 741.
57. R. HAUPT AND L. WENDLER, *Zeitschr. f. Physik* **B94** (1994), 49.